CHAPTER IV
RESULTS AND DISCUSSION

4.1 Catalyst Characterization

4.1.1 Surface Area Measurement (SAA)

The catalyst surface area was determined quantitatively as a function of loading of Nickel over NaY. Physisorption of N_2 molecules using multiple point BET method was employed to measure the surface area. The catalyst prepared by two different techniques; incipient wetness impregnation and cation-exchange. The BET surface areas of the calcined and spent catalysts are shown in Table 4.1.

Table 4.1 BET characterization results of the fresh and spent catalysts

Sample	% wt Ni loading	BET surface area (m^2/g)	
		Fresh catalyst	Spent catalyst[a]
NaY	0	645.46	223.72
IM-05	5	432.96	125.42
IM-07	7	394.84	73.95
IM-11	11	318.19	60.23
IM-15	15	306.15	96.23
IE-5.4	5.38[b]	567.89	470.06
IE-6.4	6.37[b]	589.69	522.08
IE-7.3	7.28[b]	524.06	327.08

* Impregnation method: IM-x and Ion-exchange method: IE-x; x denotes as wt% Ni.

[a] spent catalyst was tested for 4 h on stream.

[b] measured by AAS.

As the results, the surface area of NaY support was close to commercial NaY zeolite's specification (700 m^2/g) and was much higher than the

Ni/NaY catalysts, as shown in Table 4.1. The reasonable declination of surface area was found in higher Ni loading when it was prepared by incipient wetness impregnation method. It was caused by Ni metal covered upon the surface of NaY. The more loss of surface area appeared upon the higher Ni content. For the catalyst prepared by different way; ion-exchange technique, higher surface area was clearly obtained unlike the trend of impregnated catalysts. Repeating ion-exchange catalyst contributed to achieve higher content with decreasing in surface area due to more amount of Ni content concealed their surface, while 6.4% wt of ion-exchange catalyst gave the highest surface area.

It was noticeable that the spent catalysts had surface area lower than the fresh catalysts as shown in Table 4.1. It may caused by the coke deposition over the catalyst surface contributed to a loss of the BET surface area. In brief, surface area had relevance to Ni contents and also different preparation. More active metal, presents at higher Ni loading, could promote the reaction. During the reaction, some carbon can be formed and deposited on the catalyst surface resulting in presence of lower surface area. Ion-exchange provided the higher surface area than the impregnation even the spent catalyst.

4.1.2 X-ray diffraction (XRD)

Figures 4.1 and 4.2 present the XRD patterns of NaY zeolite and fresh catalysts severally prepared by impregnation and ion-exchange. Typically, the appearance of main reflection is the crystal phase of support, well-defined structured NaY zeolite. Further, the XRD patterns also consist of three reflections of nickel oxide (NiO) at different angles of $2\theta = 37.248$, 43.275, and 62.878° corresponding to the distinct crystalline planes of (111), (200), and (220), respectively. The XRD patterns of the impregnated catalyst are illustrated in Figure 4.1. It is observed the NiO phase created from the decomposition of nickel nitrate precursor after calcination. The peak intensity of the diffracted radiation is related to the particle size of the crystalline phase. In most cases, the width of high intensive peaks at the half-height of peak (FWHM) has been used for estimation of the crystal size of NiO. Except that high metal content and the diffraction line become broad and diffuse can

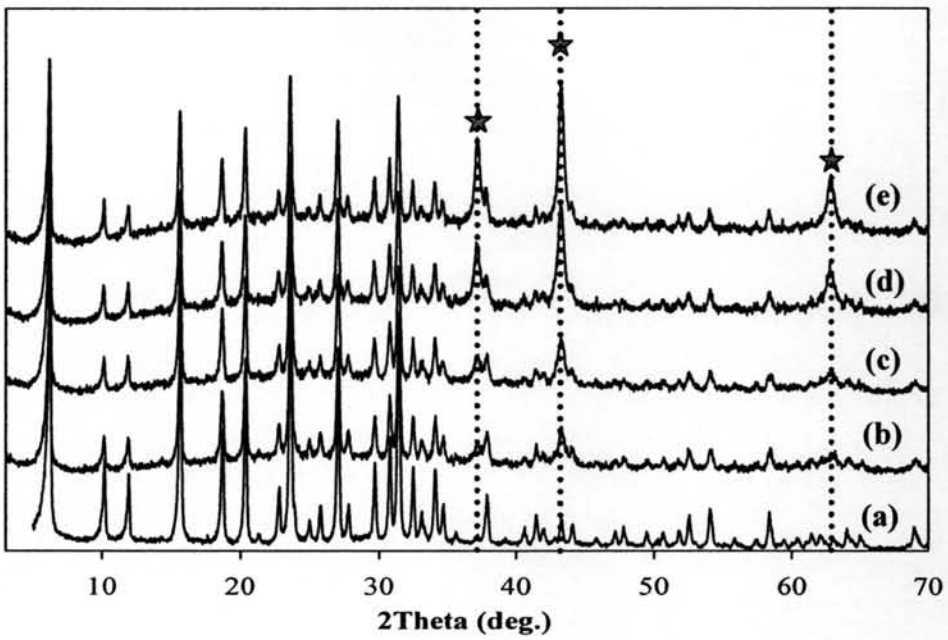

Figure 4.1 XRD patterns of NaY zeolite and calcined impregnated catalysts with different Ni loadings; (a) NaY zeolite, (b) IM-05, (c) IM-07, (d) IM-11, and (e) IM-15; where (★) denotes reflection of NiO phase.

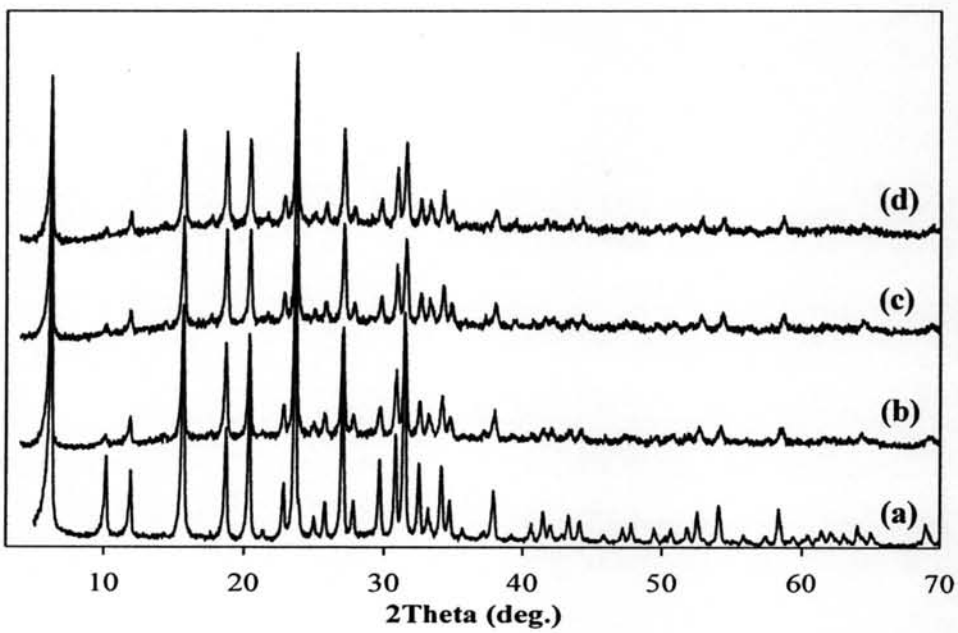

Figure 4.2 XRD patterns of NaY zeolite and supported NaY catalysts, prepared through ion-exchange technique, with various Ni loadings; (a) NaY zeolite, (b) IE-5.4, (c) IE-6.4, and (d) IE-7.3.

cause peak overlap upon the NiO phase and support intensity (Anderson and García, 2005). Therefore, it is not precise to estimate the crystallite size from Scherrer equation. However, in Figure 4.1, it was remarkable that the NiO peaks at 37, 43, and 63° of lower metal loading catalysts are weaker and broader than the catalysts with higher metal loading. It can be concluded that the NiO sizes on low loading catalysts are smaller than the catalysts with higher Ni content. In addition, it is remarkable that all metal loaded catalysts have lower intensity of crystalline peaks of NaY zeolite framework compared to the peaks of the NaY zeolite. It is indicated that the presence of NiO led to a decrease of crystallinity of zeolite as support phase. Sahli *et al.* (2006) reported resemble the XRD pattern on $NiAl_2O_4$ spinel.

The XRD patterns of ion-exchanged catalysts are presented in Figure 4.2. The catalysts were calcined at 700°C prior to be examined a diffraction pattern. As the result, no peak of NiO phase is found in this pattern. It may imply Ni^{2+} would stabilize framework of the zeolite support as exchangeable cation. This can be suggested that the preparation technique obtained different patterns of NiO phase.

Prior to catalyze in the reaction, the fresh catalysts have to be pretreated by reduction with pure H_2 at 700°C for 1 h. Figures 4.3 and 4.4 show the observed XRD patterns for the catalysts prepared by impregnation and ion-exchange techniques, respectively. It is apparent that two reflections of the Ni^0 peaks located at 2θ = 44.507 and 51.846° attributed to the different crystal planes of Ni (111) and (200), respectively. In comparison, they are observed the similar trends of two XRD patterns. The low Ni loading catalysts showed a broader and smaller peak intensity of Ni metal than the higher loading catalysts. It can be concluded that the catalysts with higher Ni content obtained a smaller crystallite size of Ni metal than the lower loading catalysts, which is in agreement with Nimwattanakul *et al.* (2006). Introduction of Ni into zeolite by ion-exchange caused a significant structural collapse of the zeolite framework corresponding to the reduction of crystallinity in Figure 4.4. The stabilized Ni^{2+} would change into zerovanlent or monovaleat form.

The comparison of XRD patterns of reduced and spent catalysts is shown in Figure 4.5. The catalysts were tested at 700°C for 4 h. Both the catalysts prepared by impregnation and ion-exchange methods also obtain the similar manner. After the reduction and reaction steps, a resemble crystallite size of metallic Ni^0 still

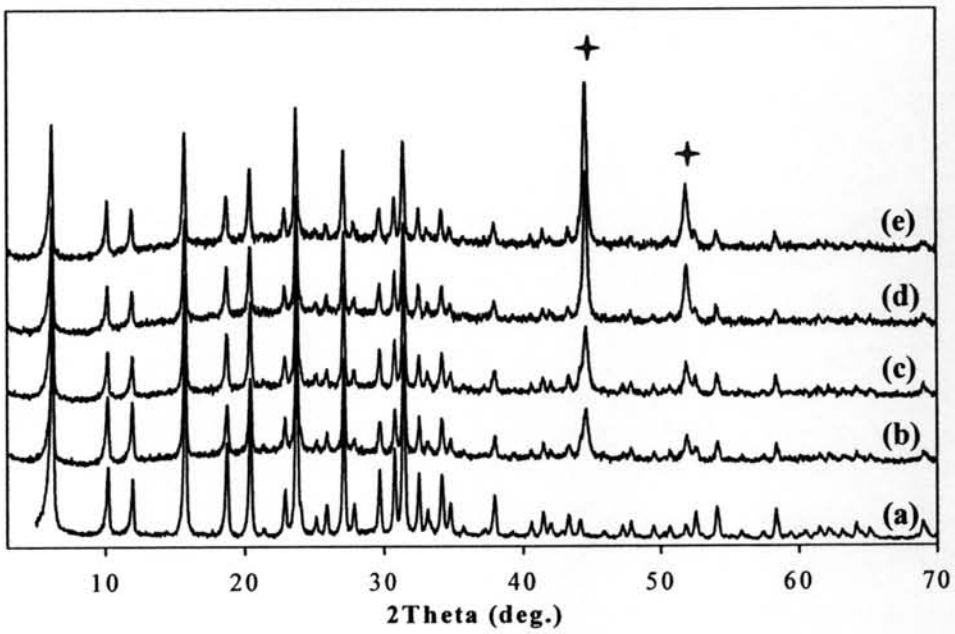

Figure 4.3 XRD patterns of NaY zeolite and reduced catalysts with various Ni contents; (a) NaY zeolite, (b) IM-05, (c) IM-07, (d) IM-11, and (e) IM-15; where (+) denotes reflection of Ni metal.

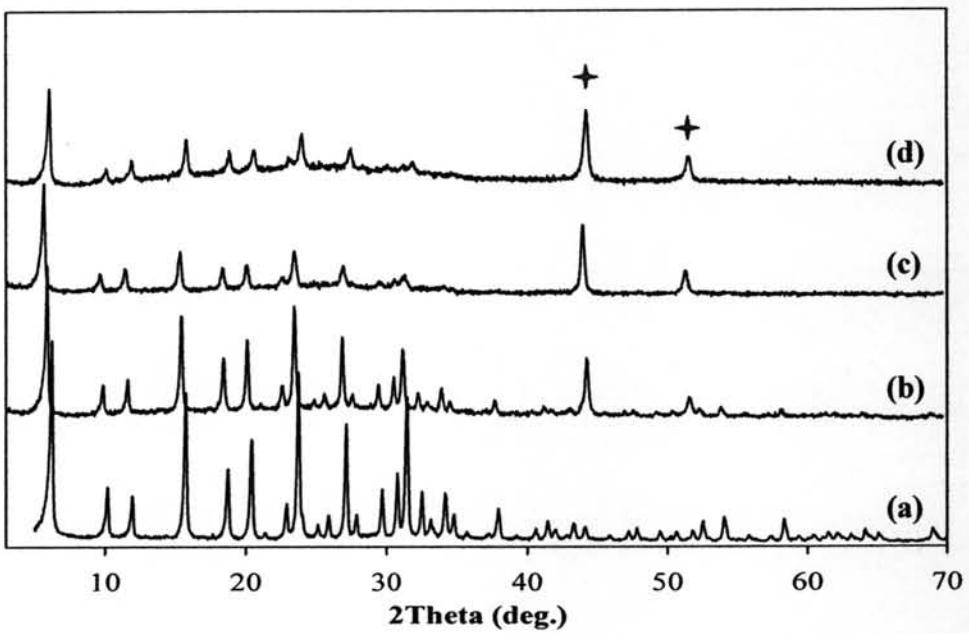

Figure 4.4 XRD patterns of NaY zeolite and reduced NaY catalysts with different Ni loadings; (a) NaY zeolite, (b) IE-5.4, (c) IE-6.4, and (d) IE-7.3; where (+) denotes reflection of Ni metal.

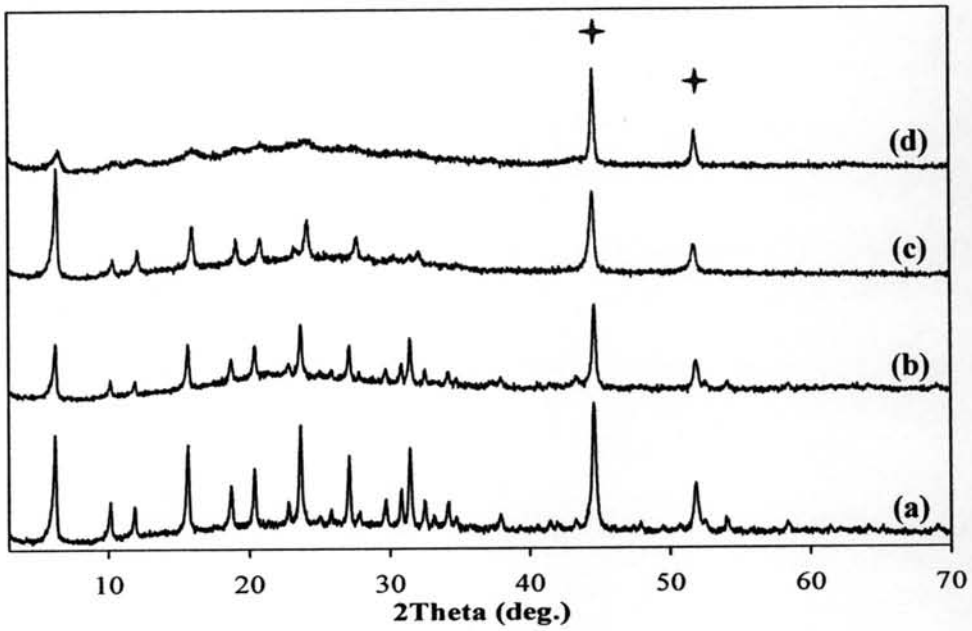

Figure 4.5 Comparison of XRD patterns of reduced and spent catalysts (a) reduced IM-11, (b) spent IM-11, (c) reduced IE-7.3, and (d) spent IE-7.3; where (+) denotes reflection of Ni metal.

presents in both of them. However, the reflection of spent IE-7.3 (curve d) has quite lower than the one of reduced catalyst (curve c). It is possible that a coke was created upon the catalyst surface. Furthermore, the comparison of fresh and spent catalysts leads to understand with sintering phenomena. The migration of individual particles occurs when exposed to a severe treatment condition such as high temperature as reported by Hughes (1984). He reported that the thermally activated process invokes from the growth of Ni crystallites and changes in particles

4.1.3 Temperature Programmed Reduction (TPR)

In steam reforming process, reduction is an essential step for preparation of metallic catalyst. To obtain active metal, the fresh catalysts were calcined at 700°C for 4 h. Following this, activation by reducing with H_2 was carried out prior to perform the reaction. A reducibility of Ni metallic was evaluated by Temperature Programmed Reduction (TPR) under 5% flow of H_2/N_2 in the temperature range of 30 to 900°C. In Figure 4.6 represents TPR profiles of the

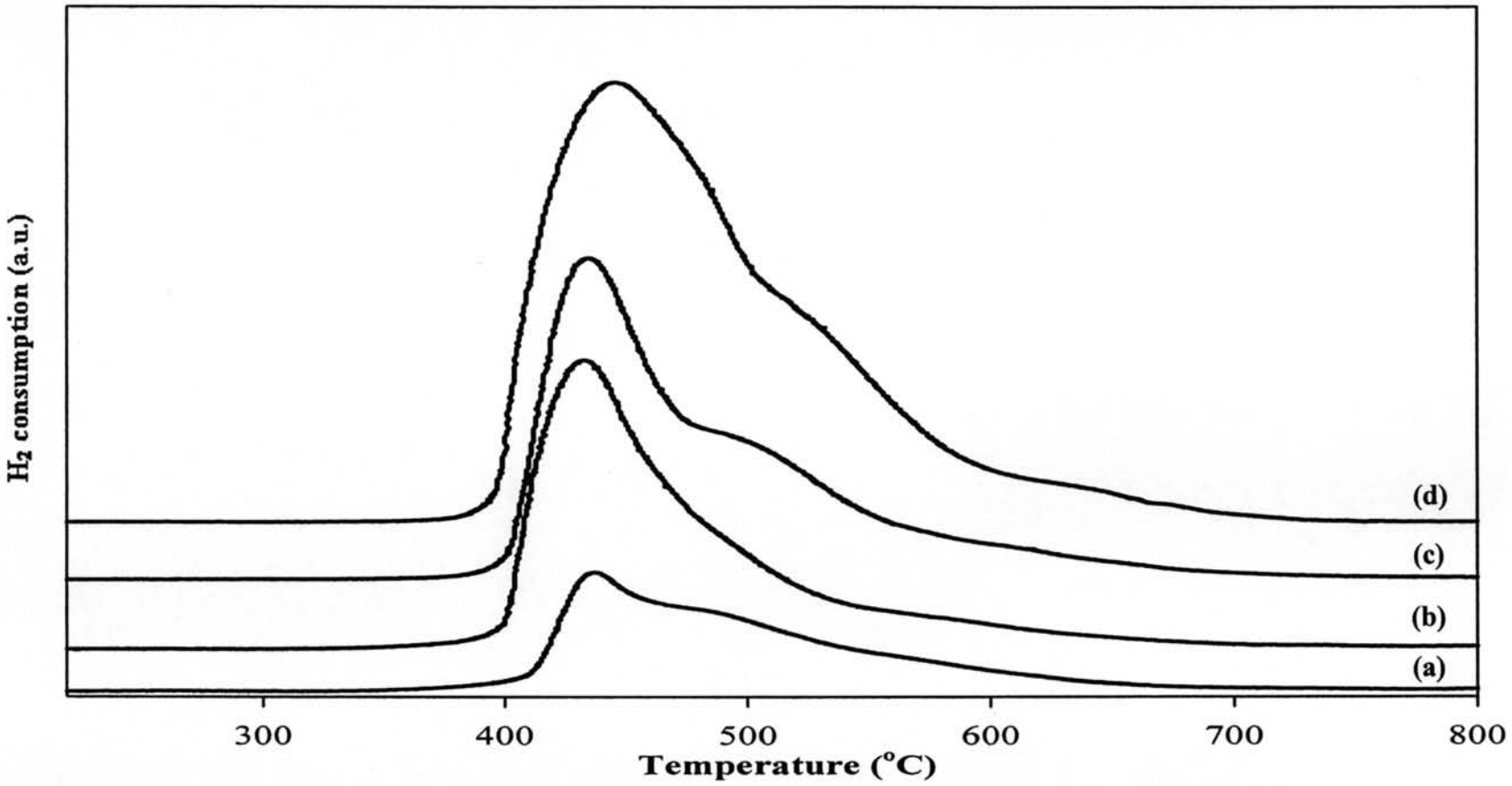

Figure 4.6 TPR profiles of the impregnated catalysts with various Ni content; (a) IM-05, (b) IM-07, (c) IM-11, and IM-15.

catalysts prepared by impregnation technique. The profiles appear the two reaction peaks in a range of 400-650°C ascribing to the stepwise reduction of NiO species at around 420°C and the humps around 500 to 620°C. This agrees with a previous research of Dong *et al.* (2001 and 2002) proposed that a sharp reduction peak of NiO presented at about 420°C in the TPR profile of the unsupported NiO. Furthermore, it is noticeable that the shift of reduction peak is observed in a different amount of Ni loadings (5-15%). In comparison, the reducibility of metallic Ni^0 is considered at the maximum reduction temperature ascending order as follow: IM-15< IM-05< IM-11<IM07. The catalyst with 15% wt Ni content showed the greatest reduction peak, while the decreasing amount of metallic loading obtained a smaller reduction peak, respectively. It may cause by the larger size of Ni^0 particles and correspond with the result from the XRD patterns in Figure 4.3.

In general, TPR profiles can observe several reduction peaks due to Ni^{2+} is directly reduced to Ni^0. The peaks appearing in the different temperature regions are attributed to the reduction of different species (Dong *et al.*, 2002). For impregnated catalysts, the sharp reduction peak appearing in the low temperature range (at about 420°C) for the catalysts corresponds to the pure NiO with small interaction with support because of the large ensemble sizes of NiO. A hump at 500°C represents the stronger interaction between metal and support. For a small hump (at 620°C) is found in profiles of higher loading catalysts containing of 11 and 15% wt Ni contents. It can be assigned to the complex of NiO_x species. This similar result had been reported by Roh *et al.* (2003) which is due to the strong interaction of support and metal and the NiO_x shoulders present over the catalysts having Ni content above 10%.

Figure 4.7 illustrates the TPR profiles of the ion-exchanged catalysts. The observation of several peaks indicated the presence of different reduction sites (Pawelec *et al.*, 2004) and having different interactions with the support. The reduction peaks are explored in the range of 300 to 900°C and compose of three main regions. The peak at the highest temperature region (maximum at 786-828) can be assigned to the reduction of stabilized Ni^{2+} species (to Ni^0 and Ni^+) having strong interaction between the active metal and the support; therefore, it is the most difficult

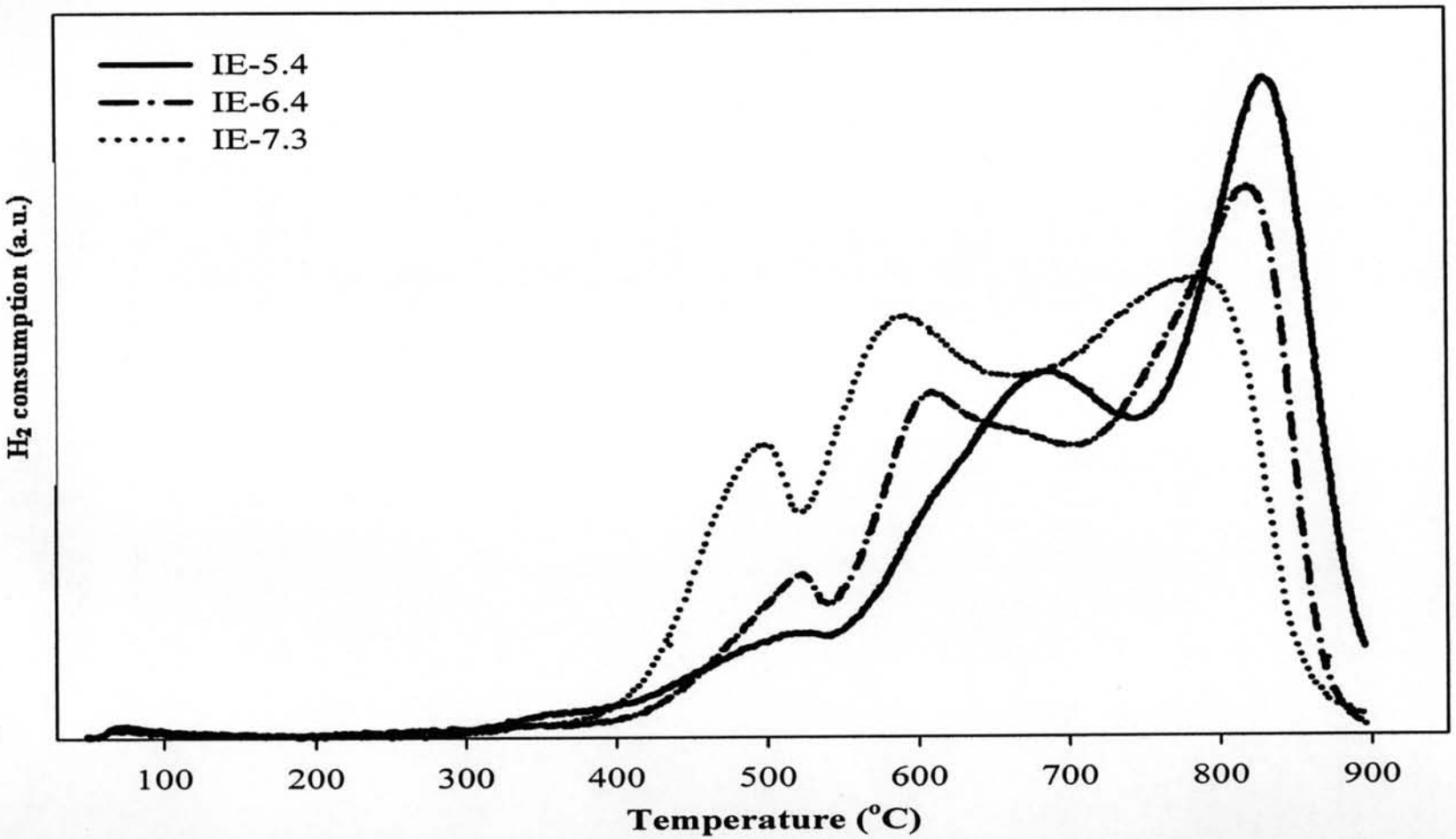

Figure 4.7 TPR profiles of the ion exchanged catalysts with various Ni content; (Solid) IE-5.4, (Dash-dot) IE-6.4, and (Dotted) IE-7.3.

to reduce into the active metal. While the appearance of reduction peaks at the middle range of maximum temperature at 590-690°C and the lowest temperature region (maximum at 786-828°C) may be due to the reduction of nickel oxide species having smaller interaction with the support, respectively. As illustrated in Figure 4.7, it is remarkable that the decreasing intensity of peaks at the highest temperature region is found and shifted to lower temperature at higher Ni content. In case of the low Ni content, the stronger interaction with support can be noticed; while the smaller interaction can be observed at higher Ni content resulting in their reducibility.

These profiles revealed the influence of methods used for introduction of metallic phase onto the support. The impregnation technique provides the distribution of active metal spread over the support. Therefore, the interaction between metal and support is weaker. For the ion exchanged catalysts, Ni^{2+} species would stabilize the framework of zeolite. This process contributes to a strong interaction with sites of zeolite support.

4.1.4 Temperature Programmed Oxidation (TPO)

Steam reforming catalyst, metallic Ni has a significant limitation on the coke formation for the period of operation. To investigate of a carbonaceous deposition then the catalysts were tested in the reaction for 4 h. Temperature Programmed Oxidation was used for evaluation of the coke accumulated on the catalyst surface under 2% O_2 in He at the temperature range of 30 to 900°C. The TPO results are given in Figures 4.8 and 4.9 which belongs to the oxidizing temperature of the impregnated catalysts and the ion exchanged catalysts, respectively. Figure 4.8, each catalyst produces two main oxidation peaks in the range of 270 to 720°C. The first peak is a hump at maximum temperature around 385°C and the appearance of oxidation peak is secondly found at maximum temperature around 675°C. The low temperature peak is due to the oxidation of non-reactive polymeric film or gum. It may caused by a slowly rate of accumulation in a circumstance of low steam to carbon ratio and low temperature at the reaction site due to a high flow rate of steam pulse according to a literature surveyed by Beurden (2004). For the coke deposited at higher temperature can be assigned to the oxidation

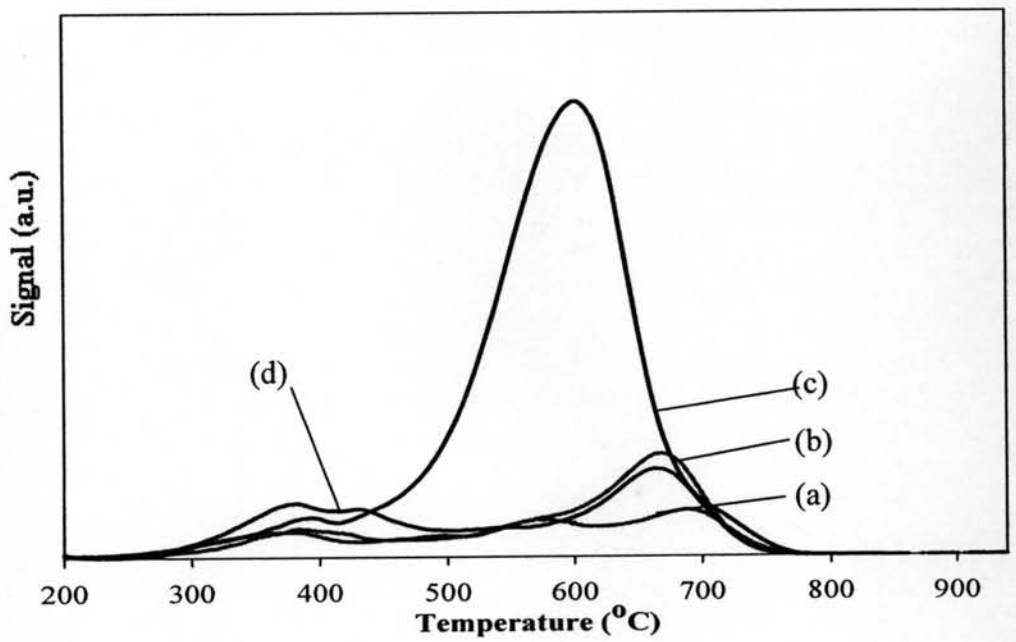

Figure 4.8 TPO profiles of the impregnated catalysts; (a,—) IM-05, (b,——) IM-07, (c,——) IM-11, and (d,——) IM-15.

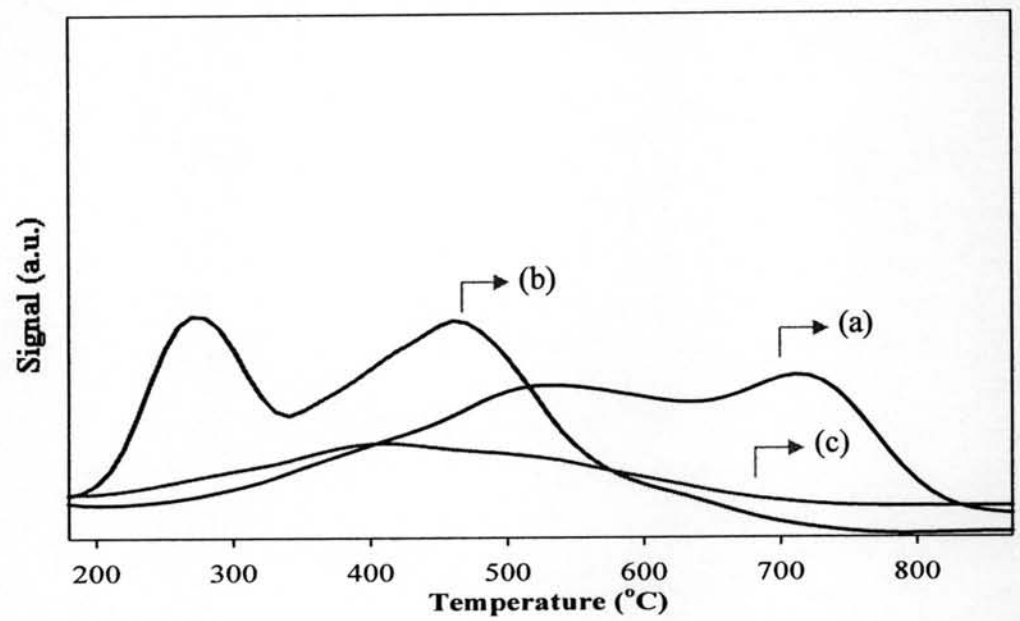

Figure 4.9 TPO profiles of the impregnated catalysts; (a,——) IE-5.4, (b,——) IE-6.4, and (c,——) IE-7.3.

peak of whisker-like carbon which is the main product of carbon formation on nickel catalysts. Trimm (1997) and Rostrup-Nielsen (1984) have reported that it involves the diffusion of gasified carbon atom through active metallic Ni. Furthermore, it is noted that the ratio between high and low temperature can imply to the relative ratio of two type of carbon. As the profiles of impregnated catalysts, the larger amount of whisker carbon is obtained comparing to the lesser amount of polymeric carbon. It probably involves the crystal size of Ni metal dispersed on support. Since the whisker-like carbon prefers to form on the large Ni crystallites, therefore it requires an enough step edge of Ni particles for nucleation. It has revealed that the critical size for carbon formation is greater than 5 nm or 10 nm. In this case, the catalysts prepared by impregnation obtained the greater Ni particles sizes than the critical size corresponding to the TEM results. It can describe the consequential TPO profiles.

Table 4.2 The oxidizing temperature of the impregnated catalysts (IM) and the ion exchanged catalyst (IE) with various loading.

Catalyst	Oxidizing Temperature (°C)
IM-05	at 378, 690
IM-07	at 388, 668
IM-11	at 393, 601
IM-15	at 380, 668
IE-5.4	at 530, 720
IE-6.4	at 270, 460
IE-7.3	at 400

As illustrated in Figure 4.9, TPO profiles of the ion exchanged catalysts is dissimilar with ones of the former catalysts. It probably related to the TPR results in Figure 4.7 which involved the distribution of stabilized Ni^0 into pore system of zeolite by using ion exchange technique. The greater amount of metallic Ni in the pore can be obtained at lower Ni content. The profiles indicated normally two oxidation peaks at different temperature range. For instance shown in Table 4.2,

the first peak of 5.4% wt of the ion exchanged catalyst appeared at maximum temperature 530°C which can be assigned to the formation of whisker carbon on the outer surface. While another peak at the maximum temperature at about 730°C attributed to graphitic carbon created in the pore of zeolite; therefore, it is difficult to oxidize these deposited carbon. In comparison, the larger amount of Ni particles on the outer surface was found with the higher loading (6.4% wt Ni content) which is easier for oxidizing coke formed. As shown in the profiles, polymeric carbon and whisker carbon can be found at lower temperatures.

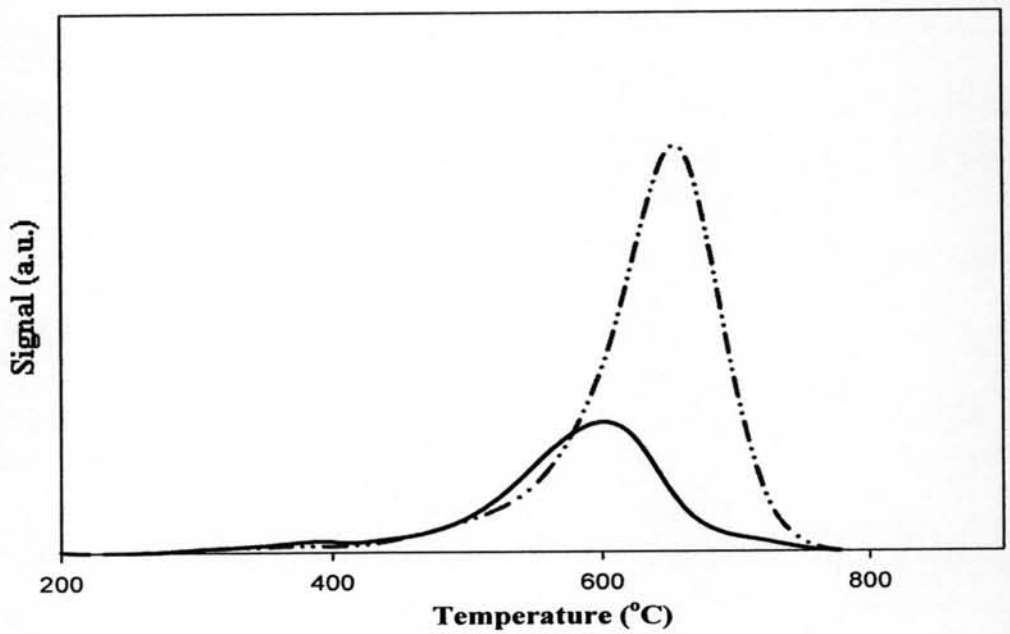

Figure 4.10 TPO profiles of different feed components; (←··–) natural gas feed and (——) methane feed.

In addition, the type of hydrocarbon contributes to the amount of coke deposition and also relates to the kind of coke formation as reported by Rostrup-Nielson *et al.* (1979). It had been reported that the steam reforming of various feedstock have limitation based on the ratio of steam to carbon. The utilization of heavier feedstocks is difficult to manipulate and caused a severe problem since it has a higher tendency to create coke and is more prone to occur deactivation. In this case, it is observed the similar results since the natural gas consists of various components

which are methane, ethane, propane, C_4, and C_5 composition. Therefore, the higher coke accumulation can be obtained by using the natural gas as feed compared to pure methane as shown in Figure 4.10.

4.1.5 Thermogravimetric Analysis (TGA)

As mentioned above that coke deposition is one of the most critical parameters that contribute to the deactivation of the catalysts. Accumulation of coke on the Ni catalysts ultimately induces catalyst deactivation due to a subsequent coverage of inactive carbon species onto catalyst surface. Thermogravimetric analysis is another technique which can be employed for estimation of the coke deposition on the spent catalysts. In all experiments, about 0.6 mg catalyst was loaded and the total rate of air flow 50 ml/min was used. The result in Figure 4.10 showed that the higher amounts of Ni content were observed the lower amount of coke formation. The activity of Ni/NaY increased with the added amount of Ni and the coke formation decreased simultaneously (from 5 to 15%). From the process of coke formation (Trimm, 1997), carbon may be gasified and may encapsulate the surface or may dissolve in the Ni crystallite. In this case, it is possible that the rate of CH_4 decomposition in higher loading and the rate of gasification are faster than the rate of carbon penetration into nickel active metal.

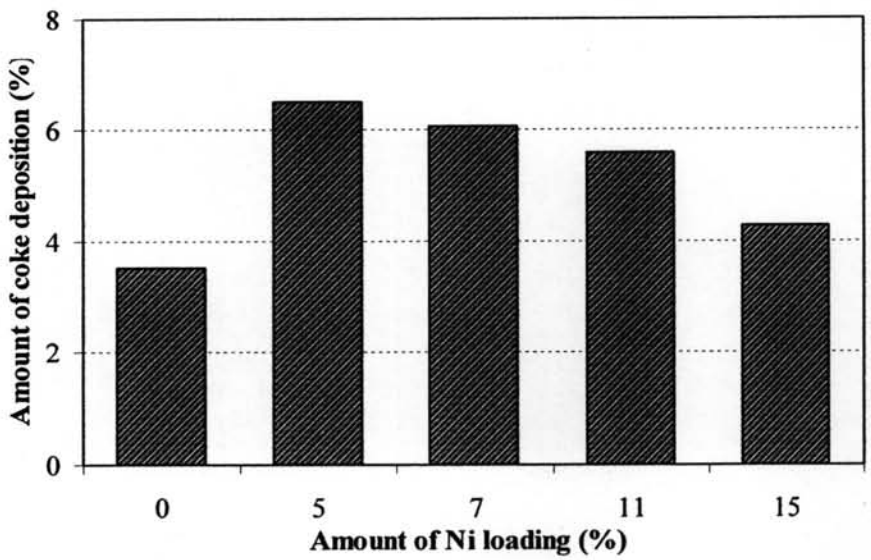

Figure 4.11 Amount of coke deposition on various Ni content catalysts.

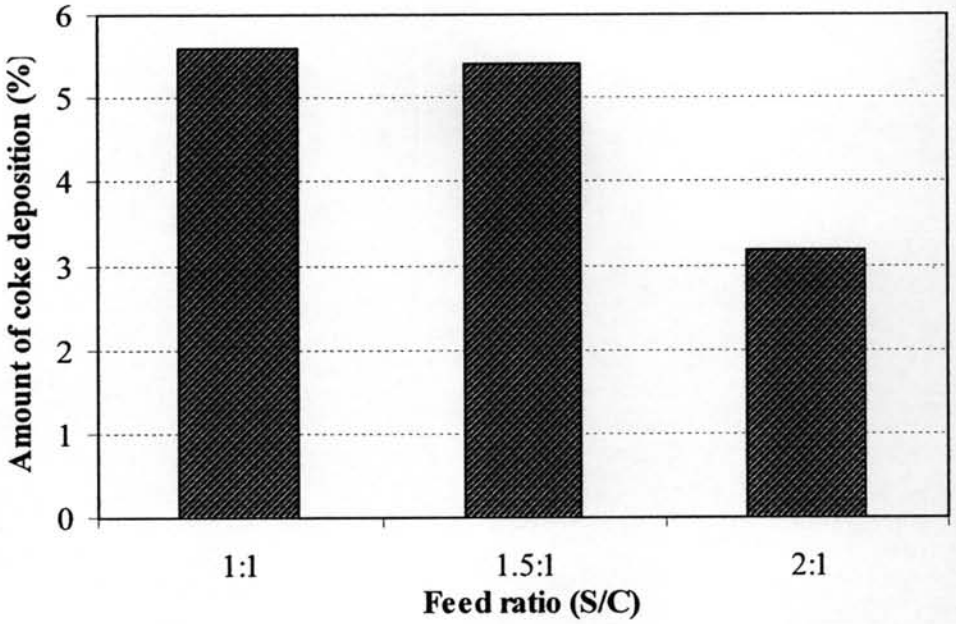

Figure 4.12 Amount of coke deposition on catalysts with various S/C ratios.

To minimize the coke formation, the ratios of steam to carbon were adjusted in the reaction at 700°C. The higher feed ratio contributes to the lesser coke accumulated on the catalyst surface. It may be due to the larger amount of steam can promote the gasification step; $C + H_2O \rightarrow CO_2 + H_2$.

4.1.6 Transmission Electron Microscope (TEM)

TEM is a direct way to roughly determine the metal particle sizes. Figure 4.13 (a) shows Bright Field TEM images of the fresh catalyst prepared by impregnation method containing 11wt% Ni content. The particle size of metallic Ni can be obtained from number of particles in each image and calculated in term of average size. As illustrated in Figure 4.13, the images present the morphology of the impregnated catalyst containing 11wt% Ni both fresh and spent catalysts for 4 h. Base on the determination, the average Ni crystallite size of the fresh catalyst is around 25.92 nm (Figure 4.13, a). After reaction at 700°C for 4 h, the change of Ni particles size can be evaluated in an average size of 30.28 nm (Figure 4.13, b). In this case, it is probably that metallic Ni may suffer from thermal sintering due to the presence of steam and exposure at high temperatures.

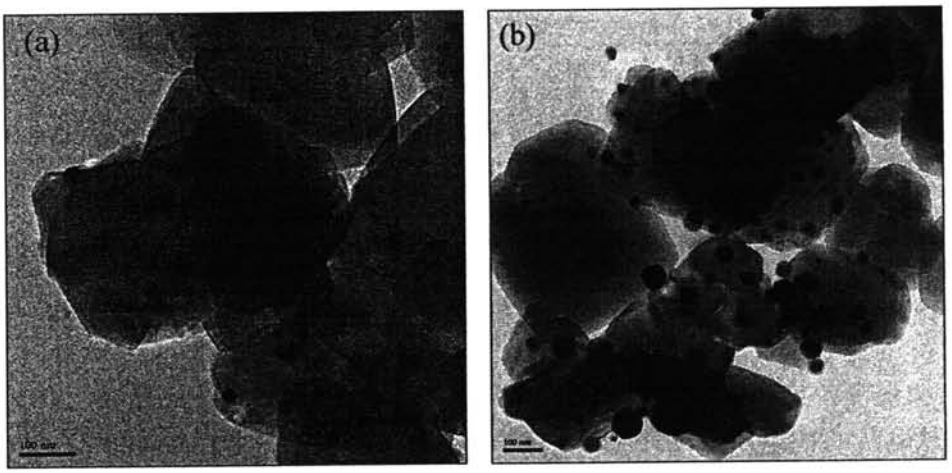

Figure 4.13 TEM images of fresh and spent catalysts; (a) fresh IM-11 and (b) spent IM-11 taken after reactivity measurements at 4 h, 700°C, S/C ratio = 1.

Furthermore, it is observed the remarkable difference on the particles size distribution of the fresh and spent 11wt% impregnated catalysts due to sintering phenomena under steam reforming reaction as shown in Figure 4.14. It is clearly seen that the size distribution of spent catalyst moves toward increasing particles size and becomes broader. The presence of significant numbers of large particles was found to be a key attribute of the spent catalyst exhibiting low activity.

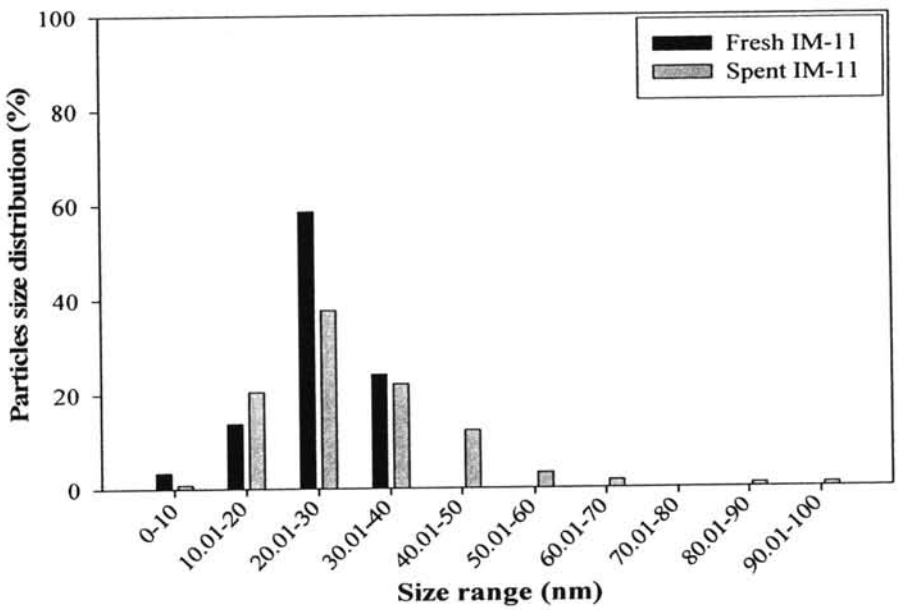

Figure 4.14 The particles size distribution (%) determined by TEM of the fresh IM-11 (dark bar) and the spent IM-11 (light bar).

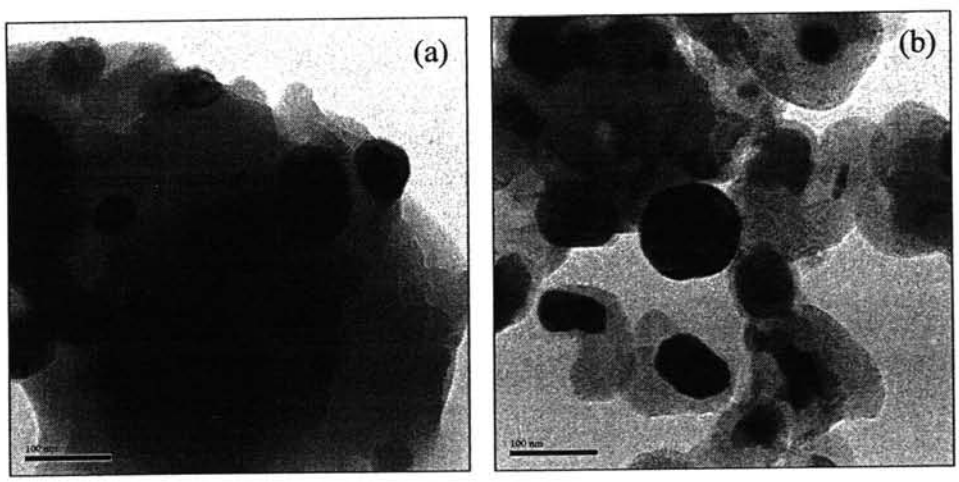

Figure 4.15 TEM images of the spent IM-11 catalysts exposed in various S/C ratio; (a) S/C =1.5 and (b) S/C = 2 taken after reactivity measurement for 4 h at 700°C.

according to the sintering. This similar result is consistent with the work reported by Carlos *et al.* (1999) that the conditions of high temperature, steam, and time on stream impact on the increasing of Ni particles size or sintering.

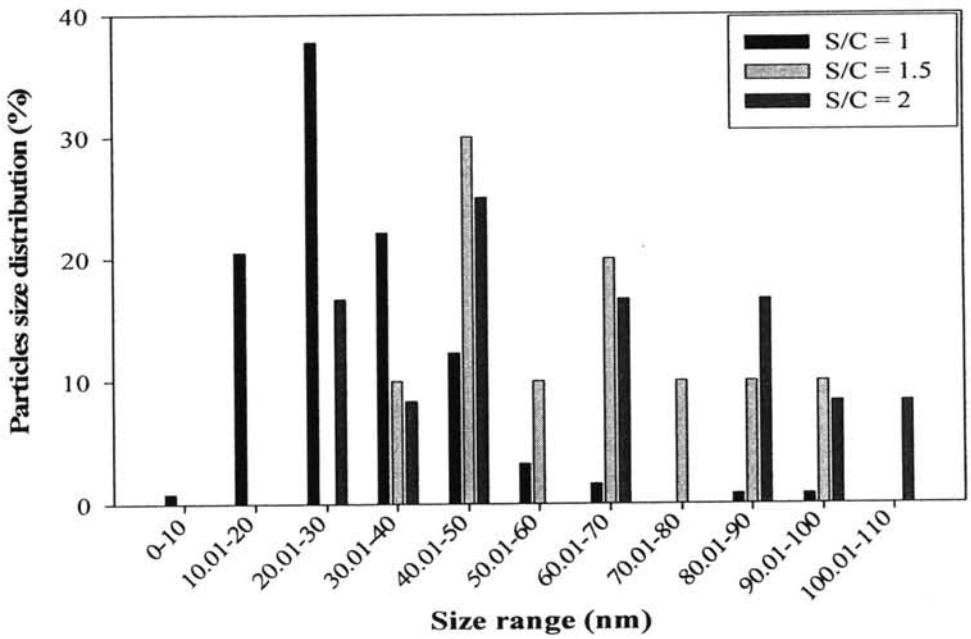

Figure 4.16 The particles size distribution (%) determined by TEM of spent IM-11 with various S/C ratios; S/C = 1 (dark), S/C = 1.5 (gray), and S/C=2 (light bar).

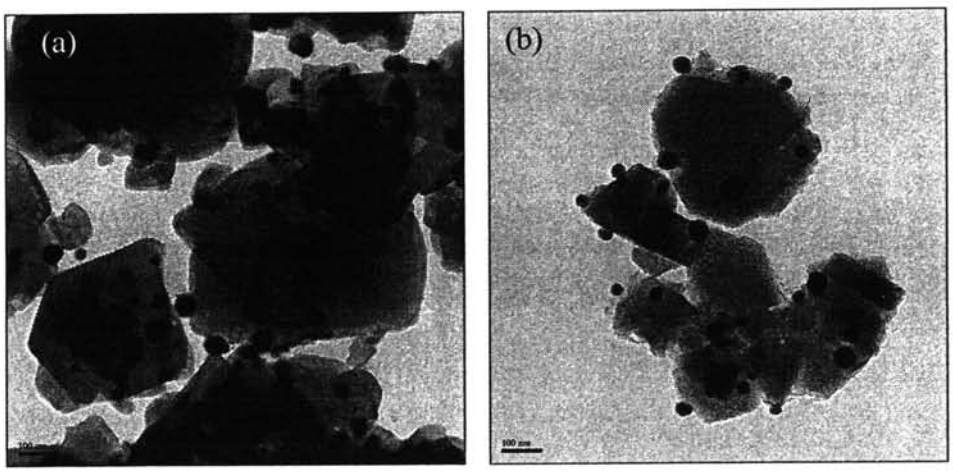

Figure 4.17 TEM images of fresh and spent catalysts; (a) Spent IM-07, (b) Spent IE-7.3 taken after reactivity measurements for 4 h at 700°C, an average Ni particle size.

Figure 4.15 shows the sintering of Ni particles due to exposure at high temperature with various S/C ratios. The average particles size is 30.28, 61.17, and 62.23 nm in the presence of S/C ratio of 1, 1.5, and 2, respectively. The result reveals that higher S/C ratio impacts on create the coalescence of Ni particles. The particle size distribution appears to be shifted towards larger particle sizes and broader range with increasing S/C ratio as illustrated in Figure 4.16.

The different techniques for introduction of metal onto the zeolite support influences to the Ni particle distribution as shown in Figure 4.17. The impregnation gave larger amount of Ni onto the surface of zeolite, while the ion exchanged catalyst obtains larger particle sizes which are about 40 nm. However, XRD pattern and TPR profiles indicated the high dispersion of a small Ni particle in pore of zeolite; therefore, it cannot be observed by TEM (Lucas *et al.*, 2005).

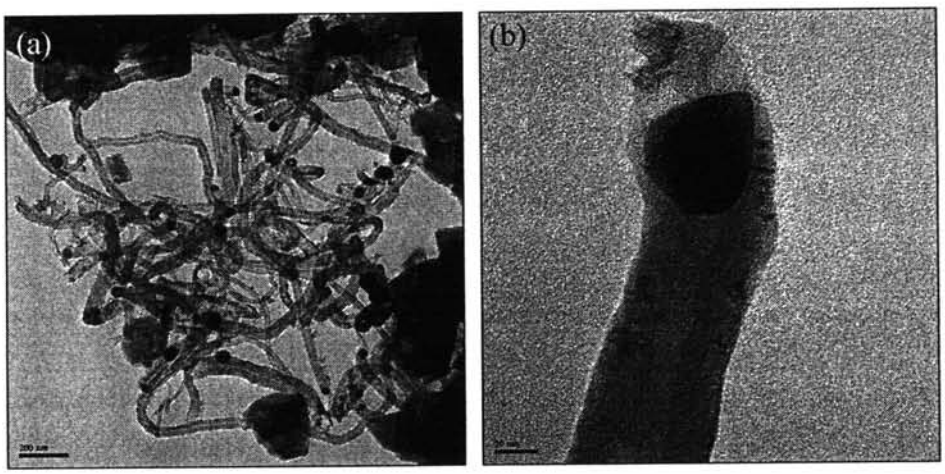

Figure 4.18 TEM images of used catalysts for 10 h at 700°C; (a) Spent IM-11 (b) carbon nanotube.

The impregnated catalyst containing 11% IM were also tested in the bench scale fuel processor at 700°C for 10 h. TEM images in Figure 4.18 illustrates that the carbon nanotube (or graphitic carbon) can be obtained for this catalyst. This type of carbon can form by the diffusion of carbon through a metal site and its subsequent precipitation as graphitic filaments. The metal plays role for coke formation. Ni, Co, and Fe metal have been reported that it is important for manufacture carbon nanotube (Lucas *et al.*, 2005).

4.2 Evaluation of catalytic activity

4.2.1 Effect of Ni loading over NaY support

The various amounts of Ni loading (5, 7, 11, and 15wt%) supported on NaY zeolite were investigated in term of the catalytic activity. The reaction was performed at 700°C under atmospheric pressure for 4 h with a steam to carbon ratio of 1. The catalysts, Ni-supported NaY prepared by incipient wetness impregnation, were used for evaluation on the effect of Ni loading on NaY support on the catalytic performance. Prior to reaction measurements, the catalysts were pretreated by H_2 with 99.99% purity at 700°C for 1 h then purged with He. The activities of the impregnated catalysts are presented in Figures 4.19 to 4.23. In term of methane conversion, it is apparent that the different amounts of Ni loading influenced on the catalyst activity. As shown in Figure 4.19, the initial methane conversion tends to increase with higher Ni contents (from 5 to 11wt%). The 5%Ni/NaY showed the initial methane conversion of 73.02% followed by the rapidly deactivation

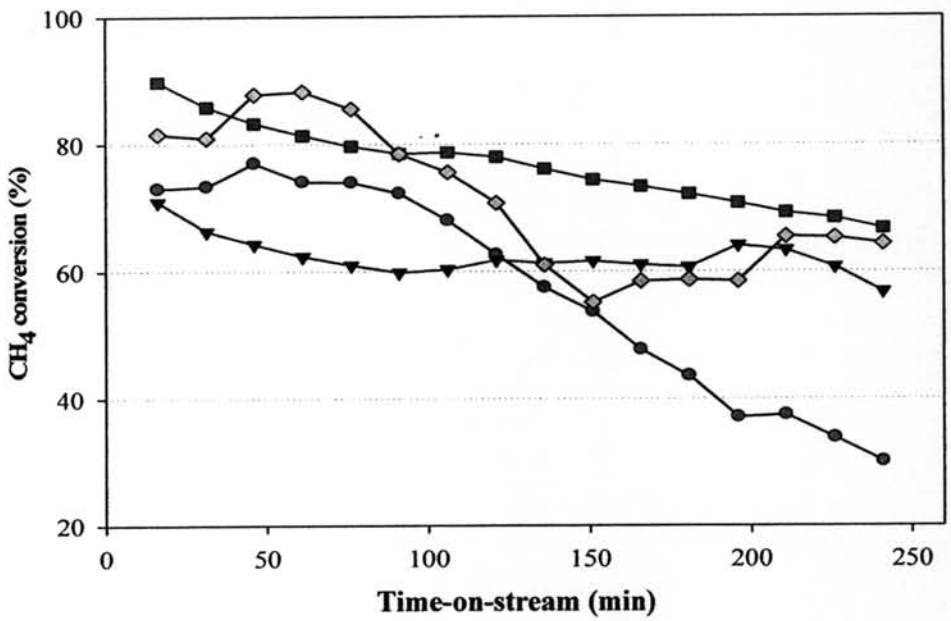

Figure 4.19 Methane conversion of the impregnated catalysts as a function of time-on-stream with various Ni loadings; (-○-) 5, (-▽-) 7, (-□-) 11, and (-◇-) 15wt% at 700°C, 1 atm, and H_2O/CH_4 ratio of 1.

within 90 min. The decreasing activity with the rate of 32.5% was found from the 5wt% catalyst with methane conversion of 30% after 240 min. The initial methane conversion of 71% was observed for the 7% Ni/NaY. Even though the initial conversion of 7% was lower than the value obtained from 5% Ni content, but the conversion of 7% rather remained constant with time-on-stream. At 240 min, it was observed the methane conversion of 56.8% with decreasing rate of 14.2%. In comparison, it is remarkably seen in Figure 4.19 that the 5%Ni/NaY exhibited higher methane conversion than the 7% at an initial stage; however, the activity of 5%Ni/NaY catalyst drastically declined. This reduction in activity of the 5% Ni could be due to high amount of carbon deposition as shown in Figure 4.11. In general, amount of metal content relates to the activity or conversion since it contains more quantities of active metal in the catalyst. At low Ni contents, the catalyst can promote the reaction for a while then the catalyst is suffered from coke deposition as the loss in activity. For 7 to 11wt% Ni, it was considered that higher Ni content affected to the increasing catalytic activity. The initial methane conversion of 89.8% was observed for 11%Ni/NaY and the conversion of 66.7% at 240 min. Finally, the highest Ni content of 15wt%, both of the initial conversion and methane conversion at 240 min is lesser than 11% which are 81.6 and 64.3%, respectively. From the results, it is indicated that the series of catalytic testing required the optimum Ni content since too high Ni content can cause the decrease in catalytic activity. Among this series, the catalyst containing 11wt% Ni/NaY exhibited the highest activity. At higher loadings, the declination of methane conversion was obtained. Base on the result, it is possible that the agglomeration of Ni particles is observed at too high metal loadings which are in good agreement with the BET surface area in Table 4.1. At high Ni contents, the surface area of the support was covered up by Ni species resulted in the loss in surface area. Besides, XRD patterns of the fresh and the reduced catalysts (Figures 4.1 and 4.2) revealed that the larger crystallite size can be obtained from higher Ni content. The agglomeration of Ni particles or thermal sintering in preparation procedure can cause the large Ni particles. These parameters impacted on the decrease of catalytic activity due to the kinks or terraces of Ni atoms involving the reforming mechanism reduced in larger particle sizes (Sehested, 2006).

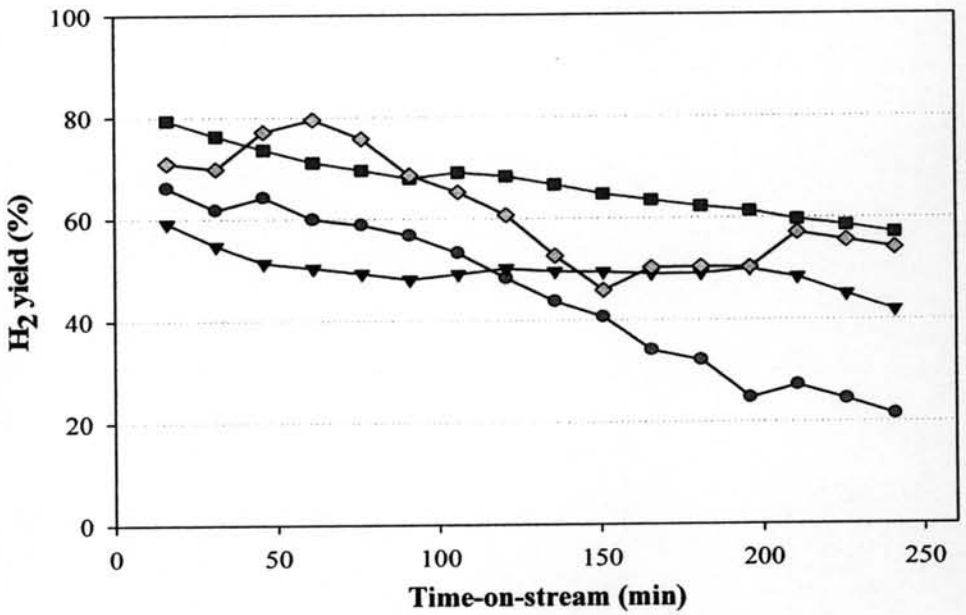

Figure 4.20 H_2 yield of the impregnated catalysts as a function of time-on-stream with various Ni loadings; (-○-) 5, (-▽-) 7, (-□-) 11, and (-◇-) 15wt% at 700°C, 1 atm, and H_2O/CH_4 ratio of 1.

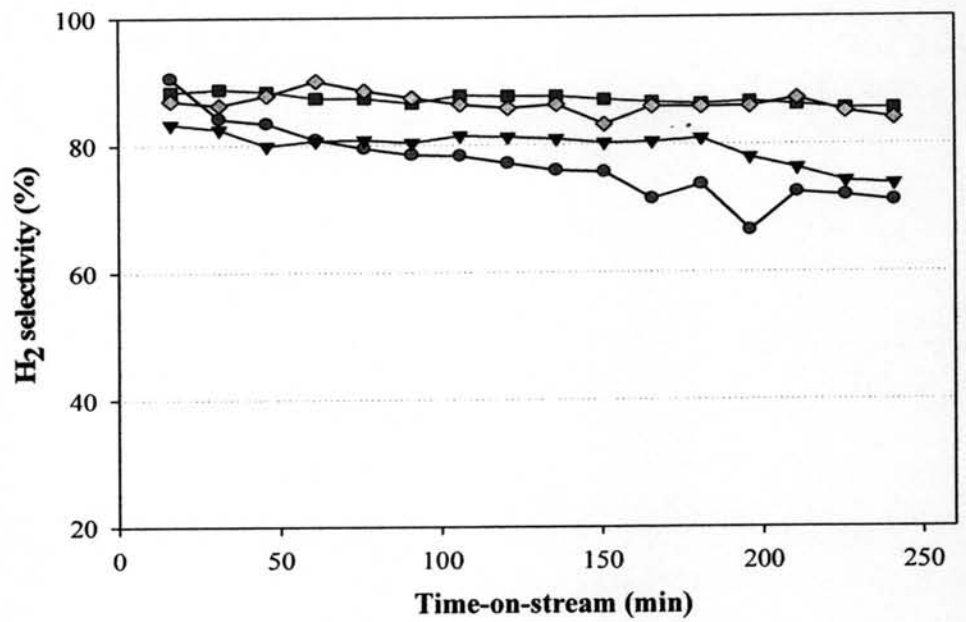

Figure 4.21 H_2 selectivity of the impregnated catalysts as a function of time-on-stream with various Ni loadings; (-○-) 5, (-▽-) 7, (-□-) 11, and (-◇-) 15wt% at 700°C, 1 atm, and H_2O/CH_4 ratio of 1.

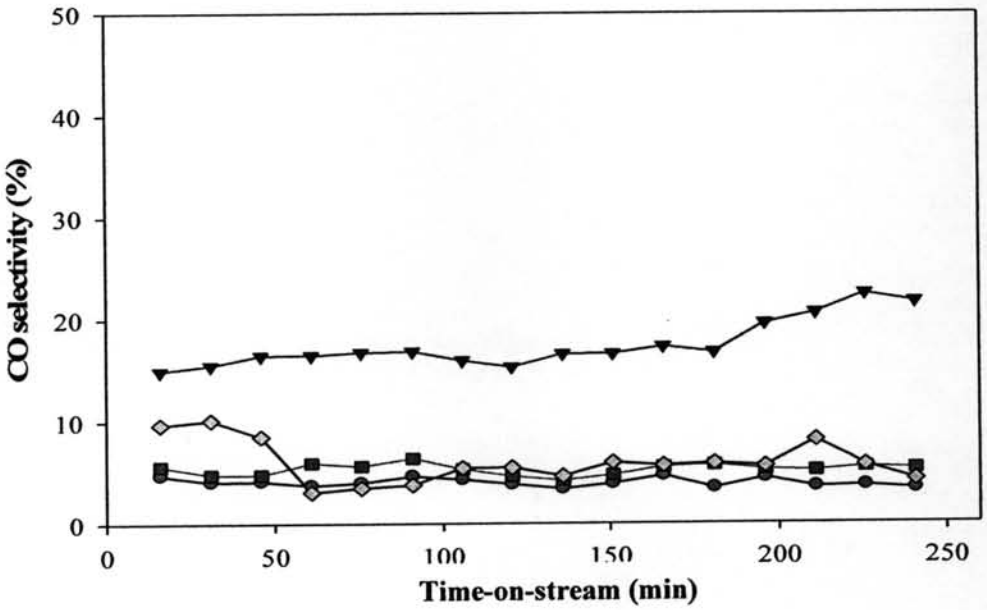

Figure 4.22 CO selectivity of the impregnated catalysts as a function of time-on-stream with various Ni loadings; (-○-) 5, (-▽-) 7, (-□-) 11, and (-◇-) 15wt% at 700°C, 1 atm, and H_2O/CH_4 ratio of 1.

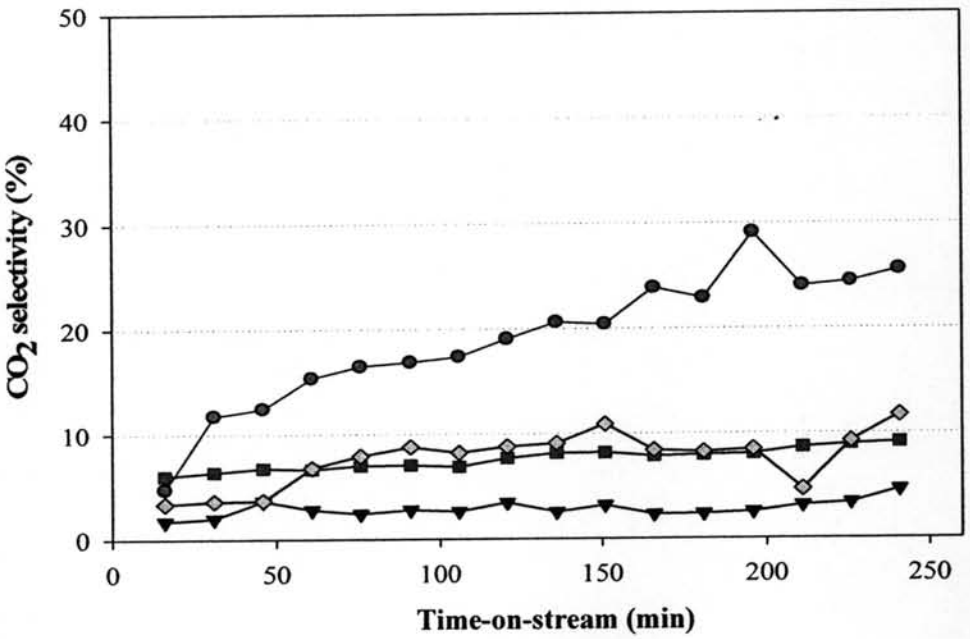

Figure 4.23 CO_2 selectivity of the impregnated catalysts as a function of time-on-stream with various Ni loadings; (-○-) 5, (-▽-) 7, (-□-) 11, and (-◇-) 15wt% at 700°C, 1 atm, and H_2O/CH_4 ratio of 1.

Figure 4.20 presents the changes of hydrogen yield as a function with time on stream. It was observed the similar trend of methane conversion and hydrogen yield due to hydrogen yield was defined as function of methane conversion and hydrogen selectivity. The changes of hydrogen selectivity are presented in Figure 4.21. For instance, the 5% showed the declination of hydrogen selectivity and hydrogen yield with time-on-stream corresponding to the methane conversion. In term of CO selectivity, it was found a relation to the CO_2 selectivity or CO_2 product generated from the side reaction, water-gas shift reaction. As shown in Figures 4.22 and 4.23, the CO selectivity of 5wt% catalyst is below 4.7% at the beginning then the selectivity showed a slightly decrease with time-on-stream. The increment of CO_2 selectivity with time-on-stream was observed in Figure 4.23. It is indicated that beside the steam reforming reaction, water-gas shift reaction (WGSR) can be observed as seen the inclination of CO_2 selectivity. Further, it is also probably that methane decomposition and gasification may associate in these reactions. In methane decomposition requires the metal catalyst to break the C-H bonds of the methane molecule into H_2 and carbonaceous as products. The carbon deposition on the surface reacts with steam producing CO_2 in gasification process later. At 5wt% Ni, it obtained larger amount of coke formed on surface due to these reactions corresponding to the CO and CO_2 selectivity. Higher amount of Ni contents tended to give lower carbon deposition as shown in TGA result (Figure 4.11) corresponding to the CO selectivity. The higher metal loading catalysts (11 and 15wt%) showed a lesser CO selectivity and greater H_2 selectivity than the lower loading catalysts. It is probably that the rate of reaction is faster than the rate of carbon atom penetrated through the metal site (Trimm, 1997). Therefore, the 11 and 15wt% gave the highest H_2 selectivity which remained constant with time-on-stream and lesser in CO selectivity. In summary, the optimum loading should be the 11%Ni/NaY catalyst as noticed from its activity compared with other catalysts with 89.6% methane conversion, 88.4% H_2 selectivity, 79.4% H_2 yield, and 5.6% CO selectivity.

From that point, the 11wt% Ni content was utilized for an investigation on the effect of steam to carbon ratio on the catalytic performance in the next section.

4.2.2 Steam to carbon ratio

The steam reforming has been used as a mature method for H_2/syngas production for several decades. The ways to improve the catalysts have been introduced over the years aimed at the reduction of catalyst deactivation suffering from three phenomena. Carbon formation is the one important factor caused the deactivation. In view point of industry, the adjustment of steam to carbon ratio (S/C ratio) is the way to overcome the limitation from carbon formation.

In this section, the S/C ratio was varied in order to determine the optimum feed ratio for the reaction. In fact, this effect was carried out on an assumption that high S/C ratio can reduce the coke formation and also provide higher methane conversion according to Trimm (1997). It has been reported that the addition of steam into the reaction is the way to minimize coke formation. Since the carbon deposited could be removed by adding higher amount of steam; therefore, the reaction should be driven forward and it could affect to the higher conversion of the reactant. To prove an assumption, the reaction was carried out at 700°C under atmospheric pressure condition. The impregnated catalyst containing 11wt% Ni content was utilized in this study. The activity with various ratios of S/C is illustrated in Figures 4.24 to 4.28. Figure 4.24 presents that higher S/C ratios impacted on the declination of methane conversion. The 11wt% with S/C ratio of 1 gave 89.8% the initial methane conversion, while the S/C ratio of 1.5 and 2 contributed to the initial methane conversion of 80.7 and 75.90%, respectively. The rate of decreased activity also related to the S/C ratio. It was found that at higher S/C ratios provided an increase of the rate of deactivation. This result is conflict with several researches in steam reforming process. Liu *et al.* (2002) reported that both methane conversion and H_2 yield are increased at high S/C ratio under low pressure investigated. On the contrary, the deactivation of the catalysts at high S/C ratio may due to the sintering of the active metal when exposed to high temperature and high amount of steam. Furthermore, it has been reported by Sehested *et al.* (2006) that the sintering of Ni catalyst involves the presence of steam to hydrogen ratio (P_{H_2O}/P_{H_2} ratio). At higher P_{H_2O}/P_{H_2} ratios, sintering was observed to be faster. The reason corresponds to the result obtained in this reaction. The higher S/C ratios contributed to the lower H_2

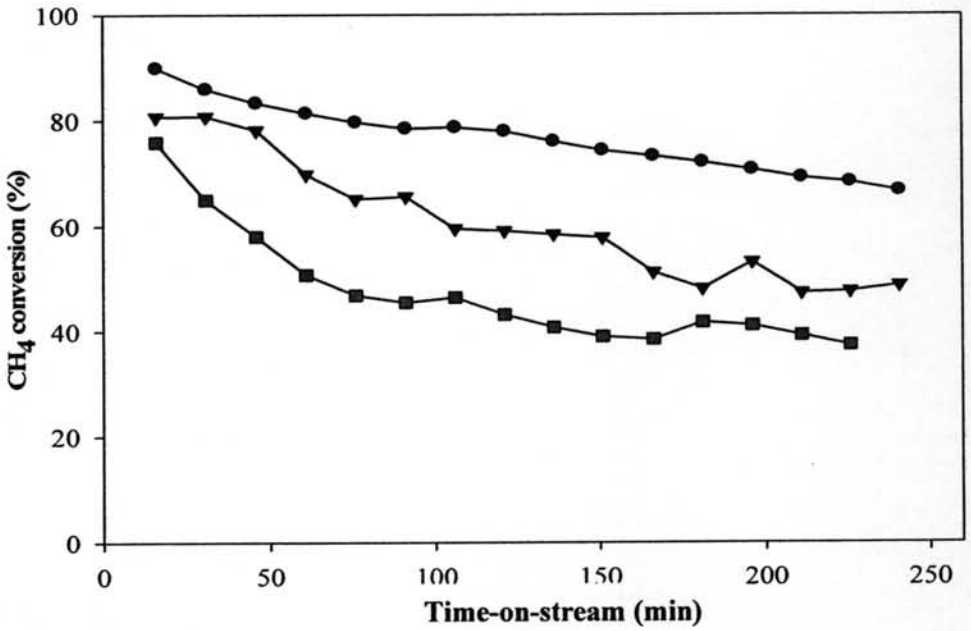

Figure 4.24 Methane conversion of the IM-11 as a function of time on stream with various feed ratios; (-○-) S/C= 1, (-▽-) S/C=1.5, and (-□-) S/C=2 at 700°C and 1 atm.

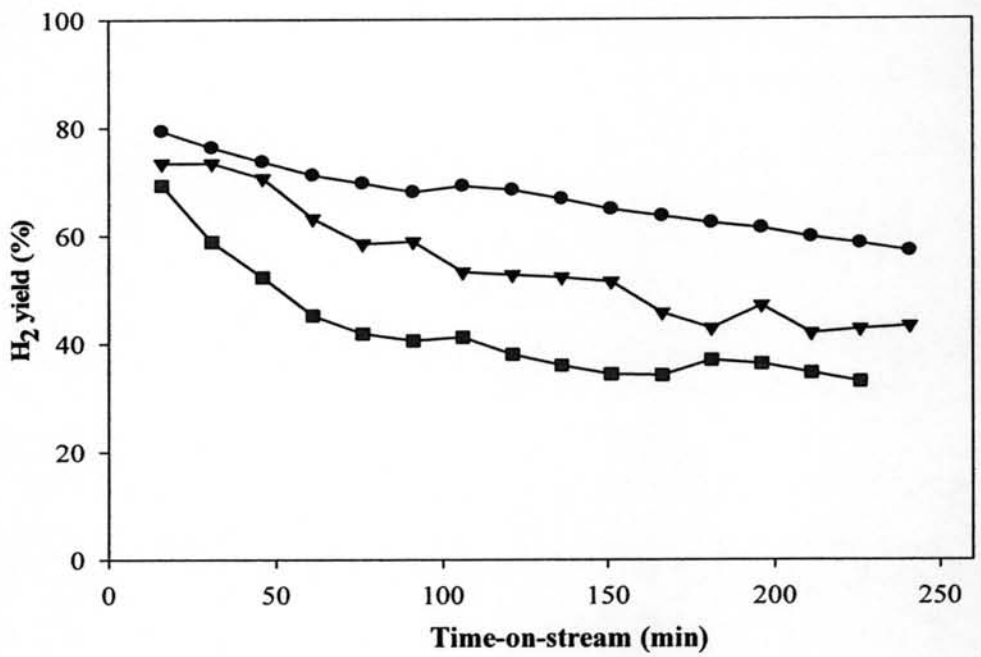

Figure 4.25 H_2 yield of the IM-11 as a function of time on stream with various feed ratios; (-○-) S/C= 1, (-▽-) S/C=1.5, and (-□-) S/C=2 at 700°C and 1 atm.

yield obtained as shown in Figure 4.25, the proportion of steam and H_2 also increased. From that point, it is probably that the catalyst suffered from the sintering of Ni metals corresponding to TEM images (Figure 4.15) which the aggregation of Ni particles is observed. The average Ni particle sizes in the presence of S/C ratios of 1, 1.5, and 2 are 31.69, 61.17, and 62.23 nm, respectively. The sintering impacted on the loss of surface area and declination of catalytic activity.

In term of H_2 selectivity as presented in Figure 4.27, the S/C ratios of 2, 1.5, and 1 gave initially 91.2, 90.9, and 88.4%, respectively. It is contrast with the CO selectivity of 2.2, 3.2, and 5.6%, obtained from the catalysts with S/C ratio of 2, 1.5, and 1, respectively. It is indicated that H_2 selectivity at high S/C ratio may be enhanced by water-gas shift reaction as also illustrated in Figure 4.26. Regarding with TGA in Figure 4.12, the amounts of coke accumulated on the surface are lesser when increasing the S/C ratio. This may be due to the enhancement of carbon removal process by gasification reaction. The two mentioned reactions can also generate higher amount of both H_2 and CO_2; therefore, H_2 selectivity is promoted in this case.

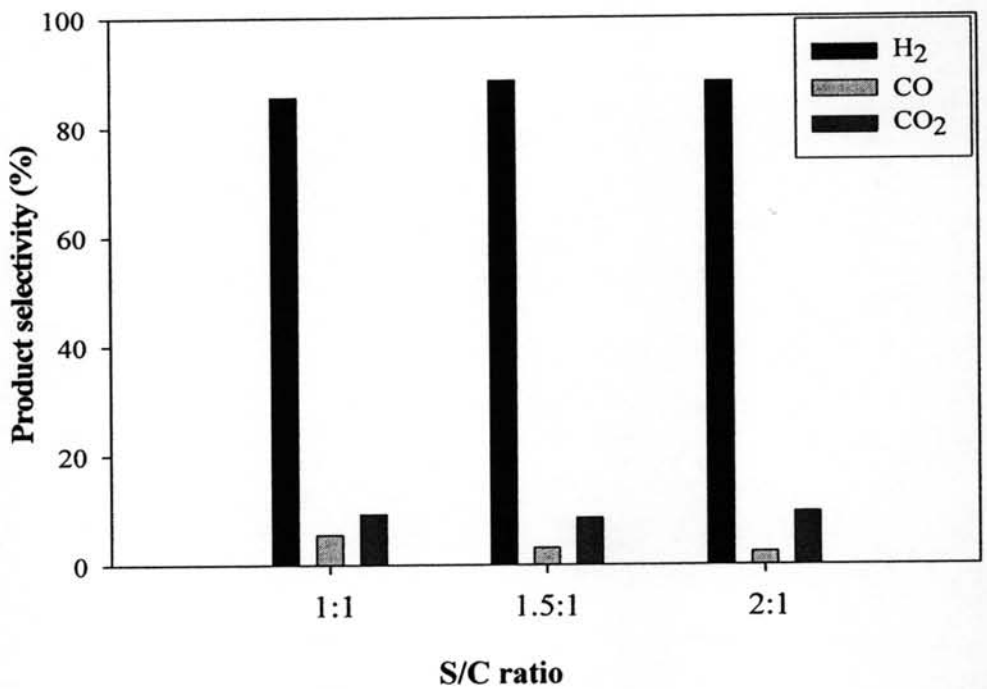

Figure 4.26 Product selectivity of the IM-11 as a function of time-on-stream with various feed ratios at 700°C and 1 atm.

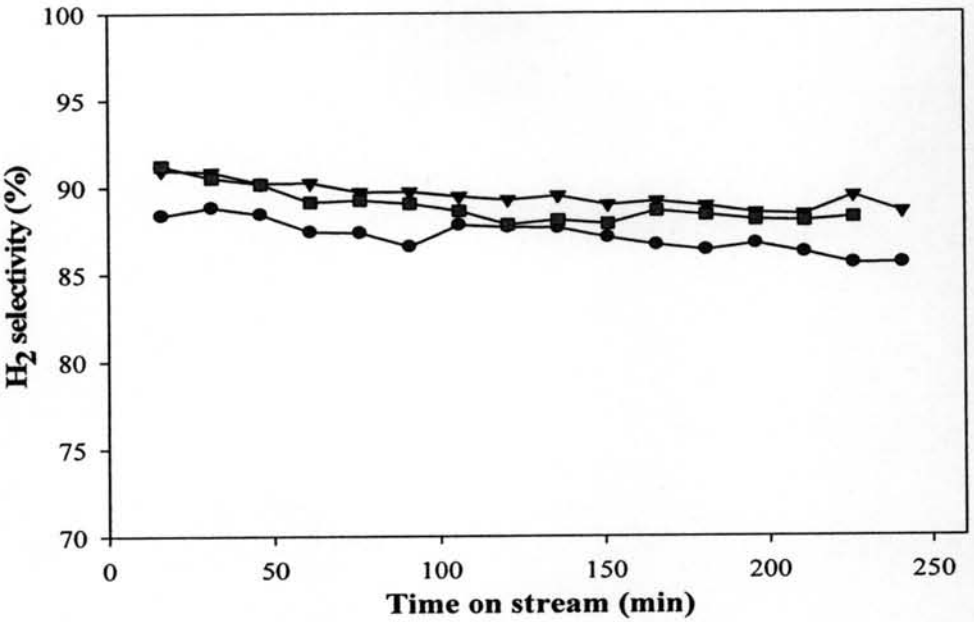

Figure 4.27 H_2 selectivity of the IM-11 as a function of time-on-stream with various feed ratios; (-○-) S/C= 1, (-▽-) S/C=1.5, and (-□-) S/C=2 at 700°C and 1 atm.

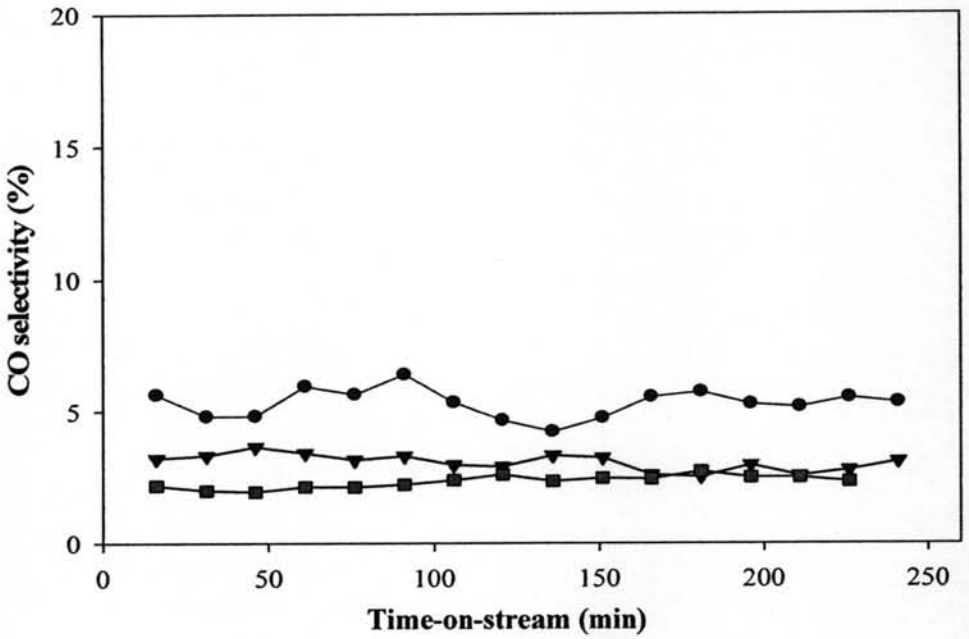

Figure 4.28 CO selectivity of the IM-11 as a function of time-on-stream with various feed ratios; (-○-) S/C= 1, (-▽-) S/C=1.5, and (-□-) S/C=2 at 700°C and 1 atm.

In the investigation of optimum S/C ratio, the deactivation of catalyst was found to be related with both sintering and carbon formation. However, it is suggested that the low S/C ratio should be used in the evaluation of the ion-exchanged catalyst activity in order to prevent the agglomerate of the Ni particles.

4.2.3 Catalytic activity of the ion-exchanged catalysts

This section involves the study on catalytic performance of the catalysts prepared by ion-exchange technique in steam reforming process. The series of the catalysts (5.4, 6.4, and 7.3wt%) was obtained by once and twice repeating cation-exchange with parent Na-exchanged Y zeolite. The experimental was carried out at 700°C, 1 atm, and a steam-to-carbon ratio of 1. The changes of methane conversion with time-on-stream are presented in Figure 4.29. As the results, the highest initial conversion of methane was observed from the catalysts containing 6.4 and 5.4wt% Ni contents, respectively. The initial methane conversions of them were 91.72 and 92.46% in sequence as shown in Table 4.3. However, the decreasing of activity was explored in these catalysts which were evaluated at 2 h. It was found that the activity of 5.4wt% Ni linearly decreased with the rate of 45.77% and the drastically decreasing in methane conversion was also found for 6.4wt% Ni content with the rate of 73.46%. While 7.3wt% of the ion-exchanged catalyst gave the lowest initial methane conversion valued at 87.17%, but the catalyst exhibited the highest stability since a slight reduction of activity was observed. Furthermore, it was noticed that the rate of decreasing activity of the ion-exchanged catalysts was lesser than former region with rate of 26.09, 13.13, and 1.72% for 6.4, 5.4, and 7.3wt%, respectively.

Table 4.3 Methane conversions with different Ni-loaded ion-exchanged catalysts.

	CH_4 conversion (%)		
	t = 16 min	t = 136 min	t = 256 min
IE-5.4	91.72	45.95	19.86
IE-6.4	92.46	19.00	5.86
IE-7.3	87.17	83.26	81.54

From these results could be related to the site of metal within the zeolite cage structure in the case of the ion-exchanged samples. The TPR profiles in Figure 4.7 also confirmed the results. The greater extent of Ni species in the ion-exchanged catalysts should be located in the pore system of the zeolite. From that reason, it is not observed a small Ni particle in TEM images. As mentioned in the

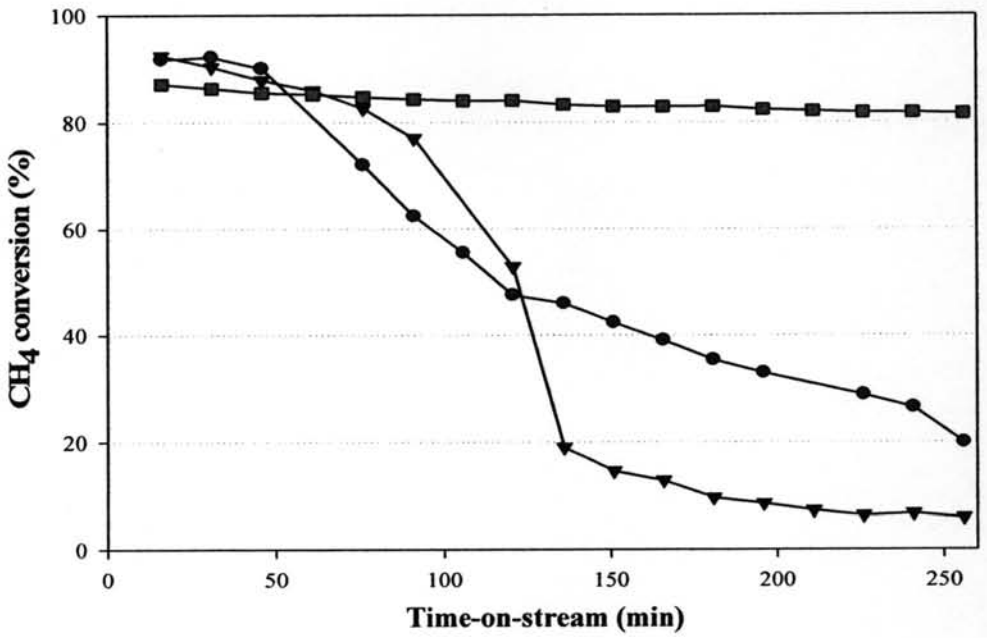

Figure 4.29 Methane conversion of the ion-exchanged catalysts as a function of time-on-stream with various Ni loadings; (-○-) 5.4, (-▽-) 6.4, and (-□-) 7.3 wt% at 700°C, 1 atm, and H_2O/CH_4 ratio of 1.

profiles that the repeating ion-exchange is the way to obtain higher loading as seen in the shift of TPR profiles to the lower temperature. On that point, it contributes to achieve different amount of Ni species located on each site of zeolite. The higher loadings provided a larger extent of Ni species to the outer surface of the support. The different distribution impacted on catalytic activity performed in steam reforming reaction.

The activity of the ion-exchanged catalysts remarkably decreased at lower Ni content since the higher proportion of Ni species could situate in the pore of the zeolite. It is noticeable that the initial methane conversions of lower Ni contents,

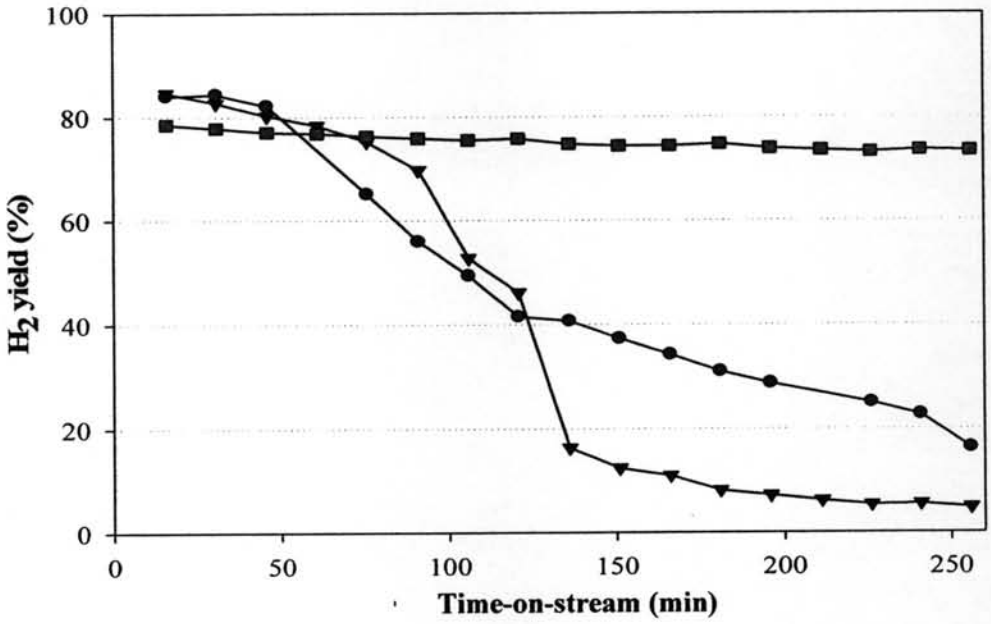

Figure 4.30 H_2 yield of the ion-exchanged catalysts as a function of time-on-stream with various Ni loadings over NaY zeolite; (-○-) 5.4, (-▽-) 6.4, and (-□-) 7.3 wt% at 700°C, 1 atm, and H_2O/CH_4 ratio of 1.

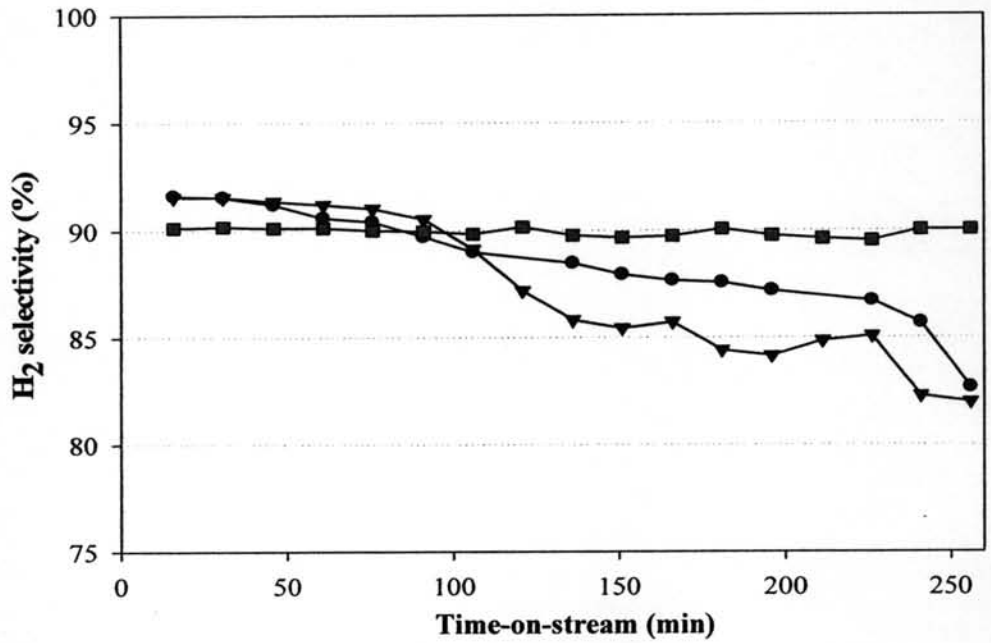

Figure 4.31 H_2 selectivity of the ion-exchanged catalysts as a function of time-on-stream with various Ni loadings; (-○-) 5.4, (-▽-) 6.4, and (-□-) 7.3wt% at 700°C, 1 atm, and H_2O/CH_4 ratio of 1.

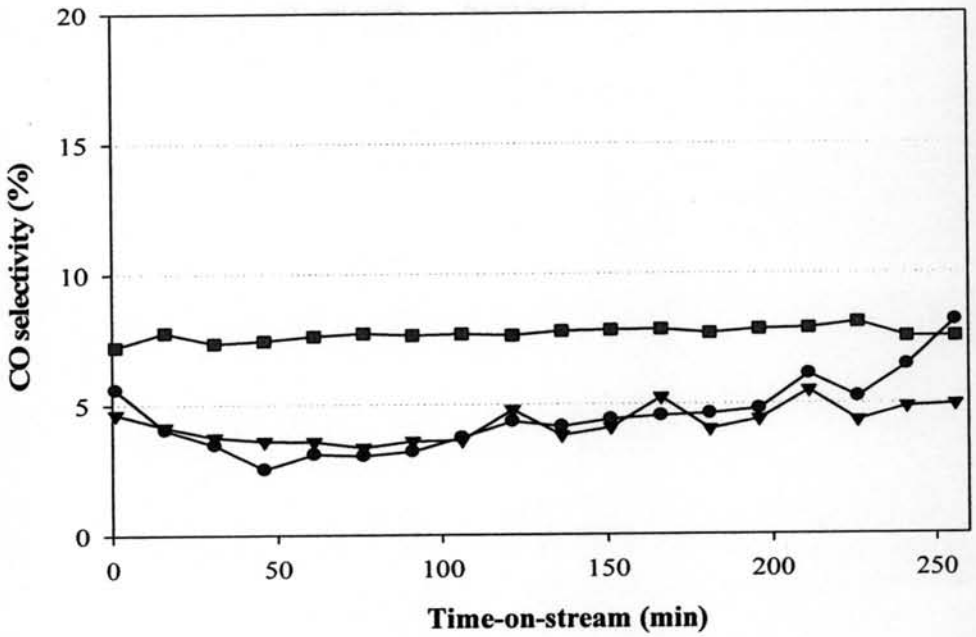

Figure 4.32 CO selectivity of the ion-exchanged catalysts as a function of time-on-stream with various Ni loadings; (-○-) 5.4, (-▽-) 6.4, and (-□-) 7.3wt% at 700°C, 1 atm, and H_2O/CH_4 ratio of 1.

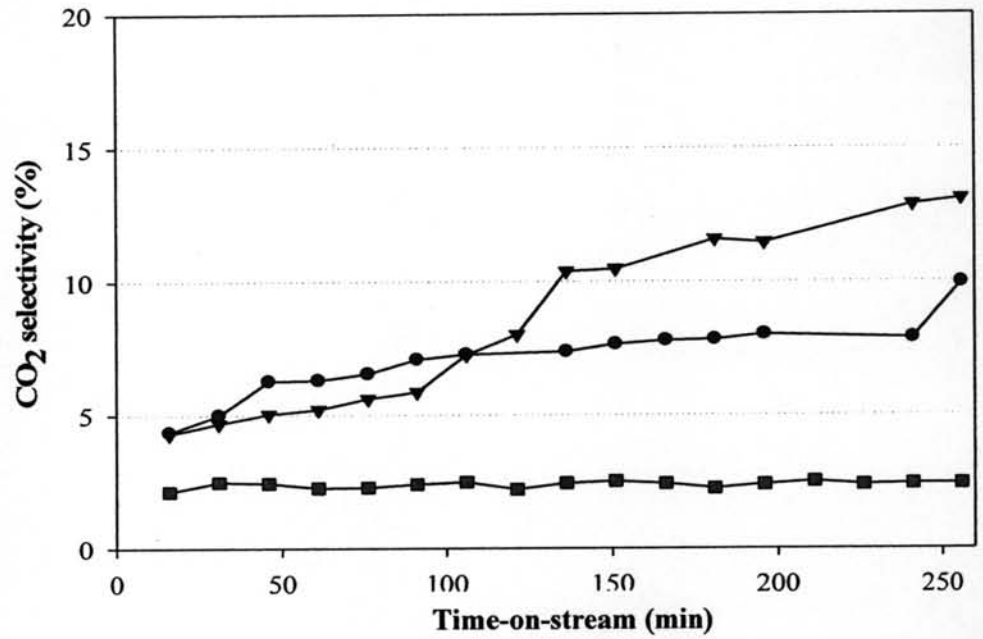

Figure 4.33 CO_2 selectivity of the ion-exchanged catalysts as a function of time-on-stream with various Ni loadings; (-○-) 5.4, (-▽-) 6.4, and (-□-) 7.3wt% at 700°C, 1 atm, and H_2O/CH_4 ratio of 1.

5.4 and 6.4wt%, are higher than 7.3wt% Ni content at the beginning. It is due to a smaller crystallite size of Ni in the pore system could promote the reaction. Then the methane conversion began to reduce faster within 50 min. In comparison, 6.4wt% Ni showed the deactivation of the catalyst which is faster than 5.4wt%. It is probably that at higher content, some of Ni species should be existed nearby the pore mouth of zeolite corresponding to the shift of the reduction temperature in the middle region as presented in TPR profiles (Figure 4.7, IE-6.4). The middle reduction peak shifts to a lower temperature affecting to easier to reduce into the Ni^0 metal. Regarding to Law *et al.* (1980), they proposed that a number of ion-exchange introduced the higher degree of acidity. The high concentration of protons in the zeolite could promote the counterdiffusion of metal cations and protons, providing more metal ions to the pore mouths. After the reduction, it became the zerovalent metal on the exterior site. In case of 6.4wt%, the coke formation, undesired product, could block the pore of zeolite contributing to faster deactivation in later region. In contrary, 7.3wt% exhibited the longer life time catalyst because of higher amount of Ni existing outside the surface. Therefore, it is less prone to deactivation caused by coke blocked in the pore system.

From that point of view, it can be summarized that the deactivation of 5.4 and 6.4wt% caused by the Ni lodge inside the pore leading to pore blockage by the coke formation. These results are similar to the rate of carbon deposition by utilizing Ni/NaY catalyst. It was reported by Lucas *et al.* (2005) that the ion-exchanged catalyst obtained the lower extent of carbon deposition caused by the coke lodged in the pore of zeolite. For 7.3wt%, higher extent of Ni on the outer surface contributes to the higher activity.

In term of selectivity as a function with time on stream are shown in Figures 4.31 to 4.33. The results revealed that the H_2, CO, and CO_2 selectivity of the ion-exchanged catalyst containing 7.3wt% Ni remained constant throughout time-on-stream. Figure 4.33 indicated that CO_2, undesired product, can occur simultaneously inhere with reformate through water-gas shift reaction. The similar direction of changes in selectivity has a relation to the degree of methane conversion as illustrated in Figures 4.31 and 4.32. The CO selectivity of 5.4 and 6.4wt% catalysts are lesser than 7.3wt%. It may be due to both catalysts are more prone to deactivate

suffering from coke formation. Therefore, it probably occur water-gas shift to generate higher amount of H_2 and CO_2 leading to achieve higher CO_2 selectivity as shown in Figure 4.33. In general, H_2 yield almost exhibits the same trend with methane conversion because it was evaluated from the methane conversion and selectivity of the catalyst. Based on the ion-exchanged results, 7.3wt% Ni is the optimum loading in this series with average methane conversion of 83.81%, H_2 selectivity of 89.95%, and H_2 yield of 75.39%.

4.2.4 Effect of feed component

In general, steam reforming on Ni catalysts in a tubular reformer is the main process for hydrogen production from natural gas. Although methane is the main component of natural gas, the gas usually also contains higher hydrocarbons. In the next part, the bench scale operation used natural gas as the hydrogen feedstocks supplied from PTT, Thailand. It composed of mainly methane and light hydrocarbon C_2-C_5. The main aim of the study is to investigate the effect of the presence of higher

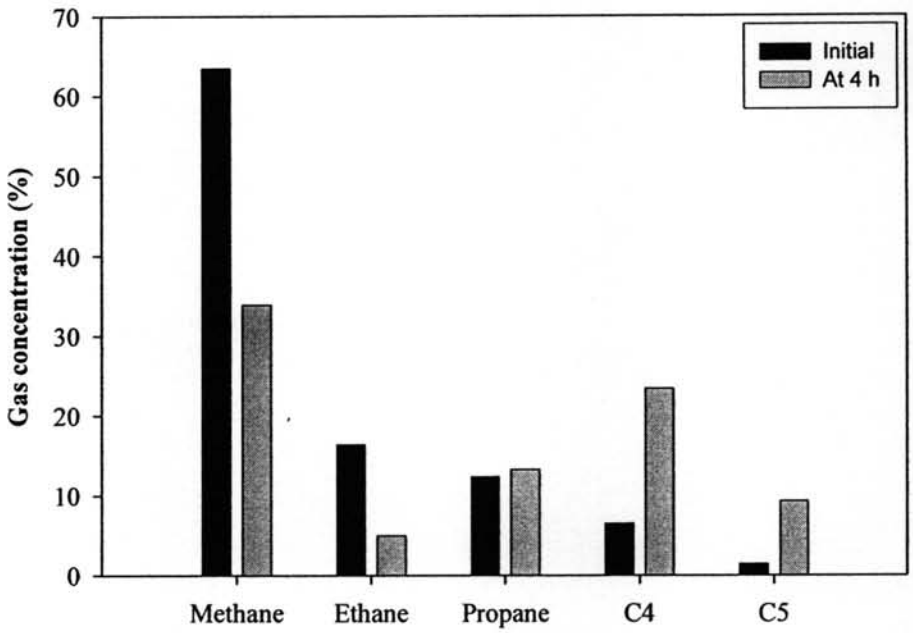

Figure 4.34 The concentration of light hydrocarbons; (dark bar) the initial natural gas component and (light bar) the reformed gas component after reactivity measurements for 4 h.

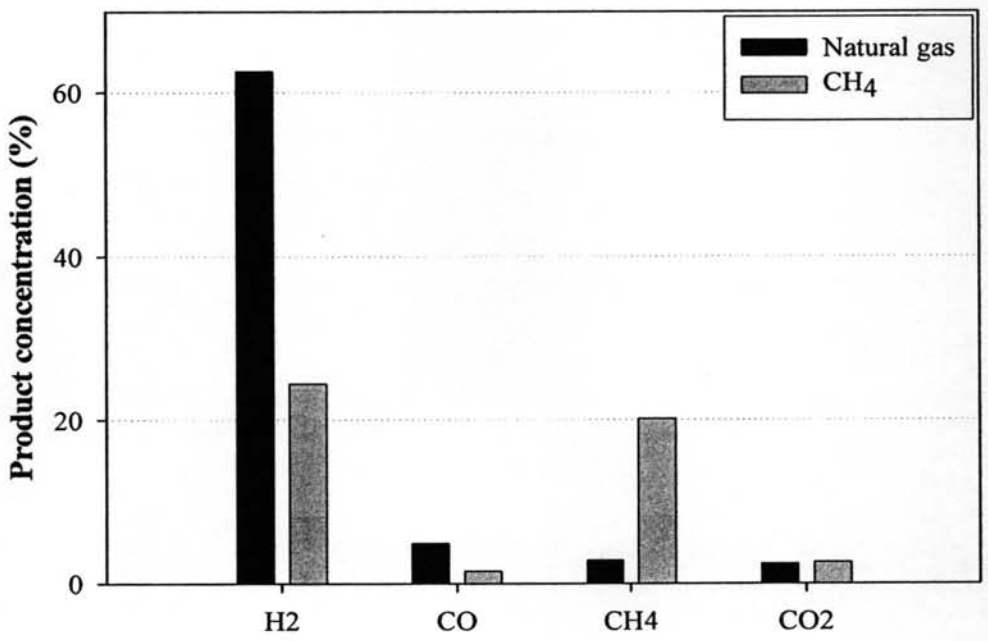

Figure 4.35 The comparison of concentration of the gas products detected at 4 h; (dark bar) the reformate in the reaction utilized methane as reactant (light bar) the reformate in the reaction utilized natural gas as reactant.

hydrocarbon on the activity of the Ni/NaY catalyst. The gas stream was tested in steam reformer with the circumstance of 700°C, 1 atm, S/C ratio=1, and GHSV=24,000 ml/g·h^{-1}. The reaction was performed with the 11wt% impregnated catalyst in order to investigate the effect of higher hydrocarbons on the Ni/NaY catalyst compared to the pure methane feed. As shown in Figure 4.34, it presents the comparison of the initial gas component and the reformate concentration which was detected at 4 h. It is observed that the concentration of methane decreased (29.5%), while the amount of the higher hydrocarbons (C_3-C_5) increased (0.9% propane, 16.9% C_4, and 7.9% C_5). This result indicated that other reactions can occur simultaneously with reforming reaction. It is probably that conversion of methane to H_2 and higher hydrocarbons can occur through dehydrogenation and rehydrogenation (methane coupling) corresponding to Garnier *et al.* (1997). With the use of group VIII metal catalysts, the conversion of methane into deposited carbon and hydrogen can completely achieve at 800°C. The short reaction period favors the carbon production and higher hydrocarbons production through the hydrogenation or

coupling from the carbon deposited. Furthermore, it has been reported that higher hydrocarbon induces the carbon nanotube formation (Otsuka *et al.*, 2003). The result corresponds to the TPO profile (Figure 4.10) which exhibited the higher amounts of coke accumulated. Figure 4.35 presents the reformate products by utilizing natural gas at 4 h. The reformate constitutes high hydrogen content of 62.6% which generate from both steam reforming and dehydrogenation of methane.

4.2.5 Bench-scale fuel processor testing

According to the aim of this part is to produce H_2 in order to approach the goal of 50 l/day. The efficiency of steam reformer in the integrated fuel processor was evaluated at 700°C under atmospheric pressure. The integrated units is combined with 4 reaction zones; a steam reformer (SMR), a high temperature water-gas shift (HT-WGS) unit, a low temperature water-gas shift (LT-WGS) unit, and a preferential oxidation (PROX) unit. Hence, the apparatus is efficient to generate H_2 at high concentrations and also achieve low level of CO content (334.83 ppm) making an advantage to utilize in PEM fuel cell applications.

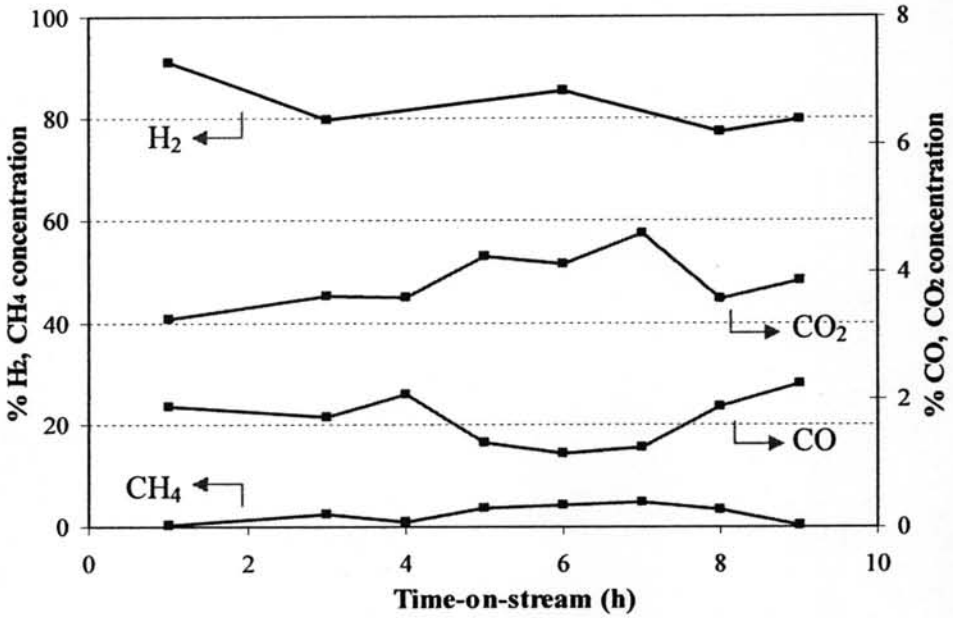

Figure 4.36 The profile of reformed gas concentration after SRM unit of fuel processor.

Table 4.4 Condition for bench-scale fuel processor testing.

Condition	SRM	HT-WGS	LT-WGS	PROX
Catalyst	11%Ni/NaY	Shiftmax 120	Shiftmax 230	Au/Na-MOR
Weight (g)	1	4.5	4.5	0.7
GHSV (ml/g·h^{-1})	4,200*	600	1200	12000
Temperature (°C)	700	450	250	200
Pressure (atm)	1	1	1	1
Feed ratio	1:1	3:1	3:1	1:1

* Dry basis

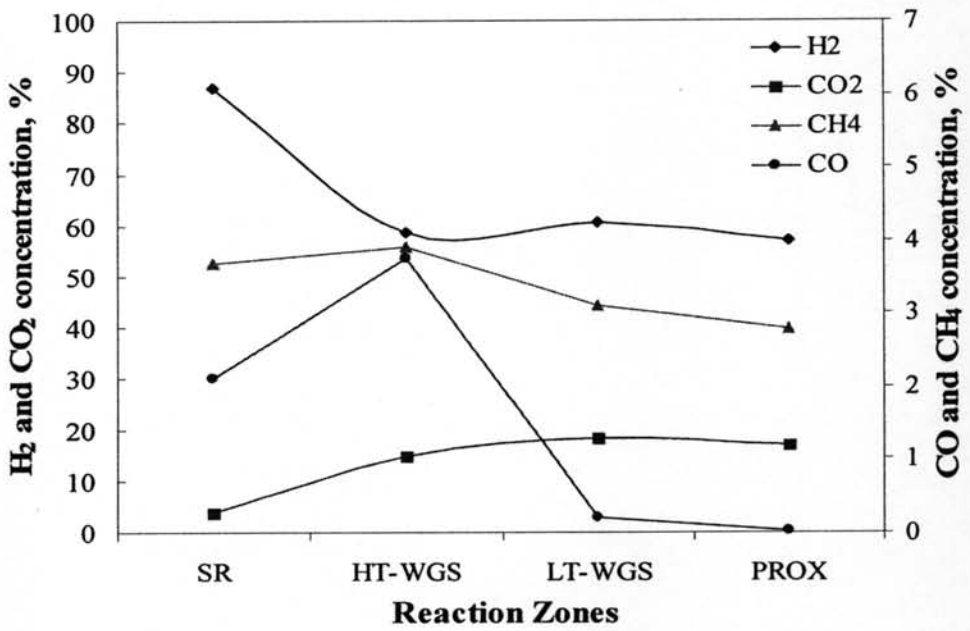

Figure 4.37 The profile of reformed gas concentration detected individual reaction zone of the integrated fuel processor.

However, only the steam reformer is focused in this thesis work. The unit plays important role in H_2 production. The impregnated catalyst having 11wt% Ni loaded was used as a reforming catalyst and natural gas was utilized as H_2 feedstock. The reaction was performed with S/C ratio of 1. The operation condition of bench-scale fuel processor testing exhibited in Table 4.4. The result in Figure 4.36 presents the capability of the reformer which generates H_2 concentration of 83.59% (76.13 l/day). The outlet reformed gas composition contains some of gas products and still remaining methane (below 5% of each gas component). In term of activity, it almostly remains constant with time on stream (9 h). Figure 4.37 demonstrates the concentration of reformed gas at 8 h. The result was detected from the individual reaction zones. It is observed that the final reformed gas has concentration of H_2 of 57.09% (90.43 l/day) which meets the goal of 50 l/day.